



OPEN ACCESS

EDITED BY

Joshuva Arockia Dhanraj,
Dayananda Sagar University, India

REVIEWED BY

Menaka Dinesh,
Sri Venkateswara College of Engineering, India
K. Lakshmikhandan,
Madanapalle Institute of Technology &
Science (MITS), India
Menda Ebraheem,
Gandhi Institute of Technology and
Management (GITAM), India

*CORRESPONDENCE

Jakeer Hussain,
✉ jakeer.hussain@vit.ac.in

RECEIVED 27 November 2025

REVISED 29 December 2025

ACCEPTED 02 January 2026

PUBLISHED 05 March 2026

CITATION

Karthikeyan U and Hussain J (2026) Hybrid animated oat Optimization–Based maximum power point tracking for small-scale wind energy conversion systems employing a SEPIC converter.

Front. Energy Res. 14:1755727.

doi: 10.3389/fenrg.2026.1755727

COPYRIGHT

© 2026 Karthikeyan and Hussain. This is an open-access article distributed under the terms of the [Creative Commons Attribution License \(CC BY\)](https://creativecommons.org/licenses/by/4.0/). The use, distribution or reproduction in other forums is permitted, provided the original author(s) and the copyright owner(s) are credited and that the original publication in this journal is cited, in accordance with accepted academic practice. No use, distribution or reproduction is permitted which does not comply with these terms.

Hybrid animated oat Optimization–Based maximum power point tracking for small-scale wind energy conversion systems employing a SEPIC converter

Udhayakumar Karthikeyan and Jakeer Hussain*

School of Electrical Engineering, Vellore Institute of Technology, Vellore, Tamil Nadu, India

This study explores a novel hybrid optimization approach called Hybrid Animated Oat Optimization (AOO) to maximize power point tracking (MPPT) in small-scale wind energy conversion systems. This algorithm combines the search characteristics of the AOO with two additional steps, adaptive contraction and reseeding, to accelerate global power-point tracking when the wind changed rapidly. The Wind Energy Conversion System (WECS) presented in this study consists of a wind turbine model, a Permanent Magnet Synchronous Generator (PMSG), an exact three-phase rectifier, and a Single-Ended Primary Inductor Converter (SEPIC) to regulate a more constant DC-link voltage. The analysis includes four MPPT techniques: Perturbation and Observation (P&O), Fuzzy Logic Control (FLC), Particle Swarm Optimization (PSO), and Hybrid AOO, all examined in MATLAB/Simulink using the identical wind profile between 8 m/s and 12 m/s. The algorithms exhibit varying efficiencies; overall, the Hybrid AOO method produced the best results. The Hybrid AOO achieves a 97.02% tracking efficiency and only a ripple of 15 W and a settling time of 0.12 s. Therefore, the Hybrid AOO method provides approximately 9% higher marginal energy yield than the other tracking methods. The results of the study further proves that the high-gain SEPIC converter offers promising performance when combined with this adaptive controller, designed for a stable and cost-effective design suited for small wind energy conversion systems.

KEYWORDS

animated oat optimization (AOO), duty cycle control, fuzzy, metaheuristic optimization, P&O, power electronics, PSO, renewable energy systems

1 Introduction

In recent decades, the issue of clean energy has evolved from a concept for future development to an urgent need for action now. Many researchers and engineers are focused on reducing carbon emissions and managing growing power demand, and with the range of renewable energy sources that exist, wind energy is among the most viable. Wind energy is generally free, highly accessible, and can be generated almost anywhere the wind blows. However, due to the variability of wind, it remains difficult to extract maximum energy from a wind turbine. This is why efficient and accurate maximum power point tracking

(MPPT) control is vital within wind energy applications; through MPPT, a machine is able to approximate maximum energy extraction within a few milliseconds. Wind generation quickly gained its position in the renewable energy movement. Wind generation does not require plan or sequences of fuel (and, therefore, by change can be considered 'free') and it do not produce any emissions; wind generation provides generation for renewable energy project development internationally. Engineers have been focused on design and generation improvement for wind blade shape, generator design, and electronic controls. These steady improvements have made Wind Energy Conversion Systems (WECS) far more reliable for both connected grids and small independent setups (Borni et al., 2021; Ravi et al., 2023). Yet wind itself remains unpredictable, and that makes it hard to keep energy output steady. As small turbines appear in villages and microgrids, finding ways to capture more power from varying wind speeds continues to be an active area of study (Ravi et al., 2023).

In addressing the challenges posed by wind variability, engineers develop a method of MPPT that allows a turbine to adjust its performance continuously to respond to variations in the wind it finds itself. The objective is simple: keep the system in the aerodynamic zone where the efficiency is highest. Over the years, several method have been evaluated including Tip-Speed Ratio (TSR), Power-Signal Feedback (PSF), Hill-Climb Search (HCS), and the popular method known as Perturb-and-Observe (P&O) method (Borni et al., 2021). Furthermore, while the P&O method is frequently implemented given its low hardware cost and requirement of few sensors with reliable operation in small WECS, it also shows limitations. Historically, the P&O method reacts relatively slower to rapid changes in wind and will make small power ripples around the maximum point in wind conditions (Ravi et al., 2023; Lopez-Flores et al., 2024). In response to this issue, other methods (these methods vary including variable-step P&O, Fuzzy Logic Controller (FLC) schemes, and neuro-fuzzy hybrid MPPT controllers) have sought improved response time and tracking conditions (Lopez-Flores et al., 2024; Rashmi and Linda, 2023). Despite these advances, the real-time operation of any wind system under MPPT control fundamentally depends on the interdependence of wind profile, load variability and converter dynamics (Arabi et al., 2024). In windy conditions or during abrupt load changes, a lag in response can occur and there are potential effects of nonlinearity associated with converter design, which might reduce efficiency. Addressing the potential challenges of lag and loss of efficiency has contributed to a call for research into bio-inspired optimization strategies such as Animated Oat Optimization (AOO), Grey Wolf Optimization (GWO), Greater Cane Rat Algorithm (GCRA), Particle Swarm Optimization (PSO) to improve tracking speed, stability of the wind system, and adaptability of performance (Rashmi and Linda, 2023; Wang et al., 2025; AboRas et al., 2025).

Simultaneously, improvements to converter design are an equally important aspect to enhance performance and tracking capabilities. Improvements in both the design of generators and converters are playing an important role in increasing overall system efficiencies. PMSG has gained popularity in variable-speed wind turbine designs due to its high torque density, brushless operation, and superior low-speed performance (Pande et al., 2021; Tan and Islam, 2004). When coupled with diode bridge rectifiers

and DC-DC converter attachments, in particular, the Single-Ended Primary Inductor Converter (SEPIC), allows for operation with steady-state input currents, non-inverted output, and broad potential for control (Ali and Ahmad, 2020; Mejbel and Hassan, 2023) and also The SEPIC converter is suitable for WECS because it supports both step-up and step-down operation, allowing stable MPPT across the wide voltage variations produced by variable-speed wind turbines. SEPIC also avoids the RHP zero present in Boost converters, providing better dynamic stability and lower input-current ripple, which enhances MPPT accuracy (?). These characteristics make it highly appropriate for WECS applications. In particular, recent work in SEPIC converter design shows redesigned circuits leading to more output voltage gain and less ripple, which may favorably distinguish PMSG-based WECS from a leveled cost perspective when interfacing these systems to utility or stand-alone loads (Vendoti et al., 2025). Recent works have implemented these "smart controllers" within a SEPIC converter with promising results establishing adaptive MPPT configurations with output voltage stability and high efficiency after changes in wind speeds (Kumari et al., 2024). The SEPIC converter was chosen over a conventional Boost topology because it supports both step-up and step-down operation, ensuring stable MPPT performance under wide WECS voltage variations (Lopez-Flores et al., 2024). Unlike the Boost converter, SEPIC does not introduce a right-half-plane zero, which improves closed-loop stability and dynamic response (Vendoti et al., 2025). In addition, SEPIC exhibits lower input-current ripple, leading to more accurate and reliable MPPT tracking (Borni et al., 2021). These characteristics make SEPIC more suitable for variable-speed wind energy systems.

Figure 1 shows the overall design of the proposed WECS combined with a PMSG-based SEPIC converter and MPPT controller. The turbine captures the kinetic energy of the wind and turns it into mechanical torque, which drives the PMSG to produce variable-frequency AC power. A three-phase rectifier then converts this AC output into DC, giving an unregulated voltage that rises or falls with wind speed. The SEPIC converter smooths and regulates that voltage so the system can feed a constant supply to the load or to the grid. The MPPT algorithm, implemented through P&O or Fuzzy Logic or PSO or the proposed Hybrid Animated Oat Optimization (AOO), keeps watching the converter's input voltage and current to calculate the instantaneous power. According to how that power changes, it adjusts the converter's duty cycle in real time so the turbine continues to extract as much energy as possible. This closed-loop setup improves energy extraction, cuts down small oscillations at steady state, and makes the overall response faster.

This paper is structured as follows: Section 2 highlights the novelty and main contributions. Section 3 gives the comprehensive literature review Section 4 presents the detailed system design, including the wind turbine model, mathematical formulation of the PMSG, and analysis of the SEPIC converter. Section 5 elaborates on the methodology adopted in this study and outlines the implementation of the four MPPT algorithms Perturb and Observe (P&O), Fuzzy Logic Control (FLC), Particle Swarm Optimization (PSO), and the proposed Hybrid Animated Oat Optimization (AOO). Section 6 discusses the simulation results and comparative performance of these techniques under identical operating conditions. Finally, Section 7, 8 summarizes the main

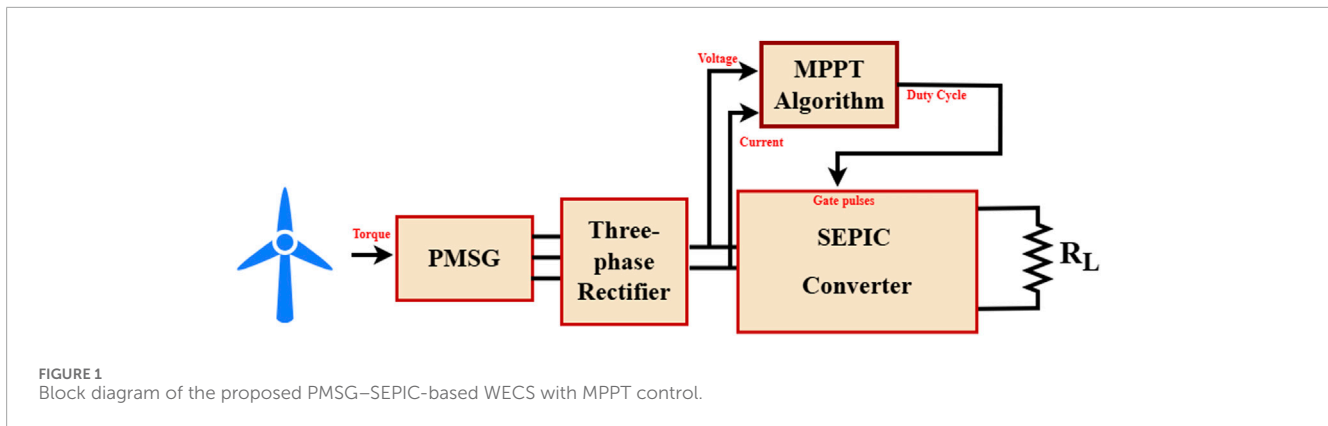


FIGURE 1
Block diagram of the proposed PMSG–SEPIC-based WECS with MPPT control.

findings, highlights the advantages of the Hybrid AOO approach, and suggests directions for future work.

2 Novelty and contributions

The key parameters of this study are the conception of a bio-inspired Hybrid AOO Algorithm in conjunction with a high-gain SEPIC converter, coupled with the design and implementation within a PMSG-based WECS. In essence, this combination offers a unified control logic to autonomously and intelligently track the maximum power point. The Hybrid AOO differs from any previous methodology, which utilized one-phase intelligent control. The Hybrid AOO utilizes a two-phase adaptive operation using a combination of re-seeding, time-varying contraction, and hygroscopic/projectile-motion operators to balance exploration and exploitation for fast convergence and stable operation even in periods of wind speed rapid variance. For this study, a complete mathematical and Simulink model was developed to link the wind turbine, electro-mechanical PMSG, and power-electronic SEPIC converter into one simulation model. This allowed us to study both transient and steady-state behavior with reasonable accuracy. In order to simulate fair Operating Conditions, a profile of wind conditions was studied in a simulation study that overall compared four MPPT methods: P&O, FLC, PSO, and the Bio-inspired numerical optimized algorithm Hybrid AOO method. The results of the finite element modeling showed that the proposed Hybrid AOO surpassed the total mean efficiency in MPPT tracking at 97.02% in efficiency compared to each testing method. Overall, the study overview proposed a new hybrid-optimization based approach for MPPT in WECS.

3 Literature review

In recent years, MPPT for WECS has evolved from classical deterministic control to adaptive and intelligent optimization. Traditional hill-climb methods such as P&O and Tip speed ratio (TSR) remain popular because of their simplicity, but they suffer from slow convergence and power oscillations when the wind speed changes rapidly (Pande et al., 2021). To overcome these drawbacks, many researchers have explored soft-computing

and meta-heuristic approaches that can deal with nonlinear aerodynamics, uncertain parameters, and converter non-linearities inherent in PMSG-based wind systems. Early intelligent MPPT research focused on FLCs, which emulate human reasoning using linguistic rules and membership functions instead of mathematical models (Borni et al., 2021). Compared P&O and fuzzy MPPT controllers for small-scale WECS and demonstrated that FLCs yield smoother steady-state behavior and faster dynamic tracking. Tests and earlier studies show that fuzzy-based MPPT methods usually react faster and adjust better when wind speed changes compared with the older, fixed-rule algorithms. They also keep the computing effort small, which makes them practical for real-time control. Still, their accuracy depends a lot on how the fuzzy rules and membership shapes are chosen, and that tuning often takes a lot of trial and error. Because of this, researchers have started mixing fuzzy logic with ideas borrowed from evolutionary computing to make the tuning automatic and more reliable (Lopez-Flores et al., 2024).

In the other hand, one method that has drawn the most attention is PSO. It's popular mainly because it's easy to understand and can search widely for a good set of control settings. In PSO, each possible group of converter parameters is treated as a small "particle" moving inside a virtual search space. The particle keeps changing its position based on its own progress and on what nearby particles have discovered. Step by step, the whole group moves toward a better common point usually the most efficient controller setup (Kennedy and Eberhart, 2021). Comparative studies have shown PSO-based MPPT to deliver faster convergence and smaller ripple than P&O while avoiding the need for gradient information (Borni et al., 2021; Ala et al., 2023). Subsequent works extended PSO to tune PI or fuzzy controllers online, achieving improved dynamic response and robustness (Arabi et al., 2024). However, the swarm's inertia and learning coefficients require careful adjustment to prevent premature convergence and overshoot during wind turbulence. The search for higher accuracy and resilience has encouraged the use of bio-inspired hybrid meta-heuristics, which combine stochastic exploration with adaptive exploitation. Algorithms such as the GWO (Rashmi and Linda, 2023), Harris Hawk Optimizer (HHO), and GCRA (AboRas et al., 2025) have been tailored for WECS to enhance tracking precision under dynamic conditions. These nature-inspired strategies mimic cooperative or physical behaviors predation, flocking, or animal

motion to locate the global MPP more reliably than single-heuristic searches. Reinforcement-learning and hybrid fuzzy-evolutionary controllers have also been reported; for instance, Reinforcement-Learning-Based Adaptive Optimal Fuzzy MPPT (Vu et al., 2022) achieved higher tracking efficiency through continuous policy updates.

Recent surveys emphasize the growing trend toward hybrid intelligent MPPT that merges meta-heuristics with converter-aware control for robustness and speed (Ravi et al., 2023; Eswaraiah and Balakrishna, 2024) reviewed multiple optimization-based MPPTs PSO, GWO, Genetic Algorithm (GA), and fuzzy hybrids and reported that combining global search and local adaptation achieves the best trade-off between convergence speed and stability. Consequently, novel algorithms such as the Animated Oat Optimization (AOO), which emulates the hygroscopic and projectile motion of oat grains (Wang et al., 2025), have emerged as promising alternatives. By incorporating time-varying contraction and reseeding mechanisms, Hybrid AOO provides self-adaptive exploration-exploitation control suitable for embedded WECS applications. Collectively, the literature reveals a clear evolution from simple perturbation techniques to intelligent and bio-inspired hybrid controllers integrated with advanced SEPIC converter architectures. Only a few researchers have actually put classical, intelligent, and hybrid MPPT methods through a fair, side-by-side test using the same wind profile and the same WECS model. Most earlier papers ran their simulations under slightly different setups, which makes comparisons tricky. Hardly anyone has looked closely at how the choice of control algorithm interacts with the converter's own behavior or how this link affects the system during fast transients and steady operation. In conclusion of the selecting of P&O, FLC, and PSO as benchmark algorithms was based on their strong presence in existing WECS MPPT research and their role as representative methods within their respective categories. The P&O technique remains the most widely used classical MPPT method and is consistently adopted as a baseline in wind energy studies due to its simplicity, low computational demand, and proven reliability in small-scale WECS (Borni et al., 2021). FLC was included because it is one of the most established intelligent MPPT approaches and has been repeatedly shown to improve dynamic response under nonlinear and rapidly varying wind conditions, making it a standard reference for rule-based, model-free MPPT controllers (Lopez-Flores et al., 2024; Vendoti et al., 2025). PSO was chosen because it represents the class of metaheuristic, population-based optimization techniques and is among the most commonly evaluated algorithms in MPPT literature for both wind and photovoltaic systems; numerous studies use PSO as a benchmark due to its strong global search capability and robustness in converter-based renewable applications (Ala et al., 2023; Arabi et al., 2024; Pande et al., 2021). Although many alternative methods exist within each category such as INC for classical approaches, ANFIS or NN-based controllers for intelligent schemes, or GA and GWO for metaheuristics these techniques either overlap conceptually with the selected algorithms, require additional sensors or training data, or provide no substantial benchmarking advantage. Moreover, including an excessive number of algorithms can dilute the clarity of comparison and distract from the main contribution of the proposed Hybrid AOO. For these reasons, P&O, FLC, and PSO offer a balanced, literature-supported, and widely accepted basis for

evaluating the performance of the proposed method in the context of WECS MPPT research. That gap is what led to the present work. In this analysis, one common simulation setup is built so that four controllers P&O, Fuzzy, PSO, and the new Hybrid AOO can be checked under identical wind conditions. Their efficiency, ripple, and response time are compared directly. At the same time, converter design has kept moving forward. Better topologies have made WECS both more efficient and easier to control. SEPIC converter has become popular in small wind systems because it gives a non-inverting output, a wide duty-cycle range, and a nearly continuous input current (Alsumiri and Althomali, 2017). Over the past few years, engineers have produced modified or cascaded SEPIC versions that use coupled inductors or switched capacitors. These versions can raise voltage roughly seven to ten times while keeping ripple and switching stress low (Mejbel and Hassan, 2023; Vendoti et al., 2025). Similar high-gain SEPIC and SEPIC-buck circuits (Emar et al., 2024; Jyothi et al., 2023) show again that converter design plays a major part in MPPT performance and that controller and converter need to be designed together. Earlier WECS mostly relied on simple boost converters, which could only increase voltage and often caused a discontinuous input current. SEPIC converters avoid those problems. They give a non-inverting output, keep the input current smooth, and cut electromagnetic noise (Alsumiri and Althomali, 2017; López Seguel et al., 2022). A basic SEPIC uses one MOSFET, two inductors, a coupling capacitor, and a diode. Because it can both raise and lower voltage, it handles the wide swings in generator output that come with changing wind speed (Sutikno and Aprilianto, 2023).

4 System design

4.1 Modeling of the wind turbine

Wind turbines play a central part in renewable-energy generation because they change the motion of air into electrical power. When the wind hits the blades, it makes them spin, and that rotation drives a generator to produce current (Karthikeyan and Hussain, 2025). The amount of power that comes out depends mainly on wind speed, the blade shape, and how well the air flows around the rotor. In practice, engineers study these factors with simple mathematical models and later test them through simulations to see how the turbine behaves under different wind patterns (Hannan et al., 2023; Stadtherr, 2019).

4.2 Mathematical modelling of the wind turbine

The power available at the shaft of the wind turbine can be described by Equation 1 (Stadtherr, 2019):

$$P_{\text{opt}} = \frac{1}{2} C_p(\lambda, \beta) \rho A V^3 \quad (1)$$

where,

ρ = air density (kg/m³)

A = swept area of the turbine blades (m²)

v = wind speed (m/s)

C_p = power coefficient.

λ = tip speed ratio of the rotor blade tip speed to the wind speed.

β = blade pitch angle (degrees)

The power that a turbine can take from the wind follows a well-known relation: it varies with the turbine's aerodynamic efficiency, the area swept by the blades, and the cube of the wind speed. This expression gives a quick estimate of how much energy a design can deliver. It also helps designers adjust blade geometry and control settings so that the system works closer to its best efficiency point (Hannan et al., 2023).

4.3 Power coefficient model

The efficiency of a wind turbine is described by the power coefficient, C_p (Stadtherr, 2019). The value of C_p changes with two parameters: the tip-speed ratio λ and the blade-pitch angle β . A commonly used empirical relationship for this dependency is given by Equation 2:

$$C_p(\lambda, \beta) = c_1 \left(\frac{c_2}{\lambda_i} - c_3\beta - c_4\beta^x - c_5 \right) e^{-c_6/\lambda_i} \quad (2)$$

where the constants depend on the turbine being modeled. For the present case, $c_1 = 0.5176$, $c_2 = 116$, $c_3 = 0.4$, $c_4 = 5$, $c_5 = 21$, and $c_6 = 0.0068$ (Hussain and Mishra, 2014).

The intermediate variable λ_i used in Equation 2 is defined as Equation 3:

$$\lambda_i = \frac{1}{\lambda + 0.08\beta - 0.035} \quad (3)$$

where, β is the pitch angle: the angle between the turbine blade and the wind direction. When $\beta = 0^\circ$, the blade lies flat with the flow, enabling the turbine to capture the maximum possible power.

The tip-speed ratio λ is the ratio of the rotor tangential speed to the wind speed and is appearing in Equations 2, 3 is defined by Equation 4:

$$\lambda = \frac{\omega_m r}{V} \quad (4)$$

where ω_m is the angular velocity of the shaft, r is the rotor radius, and V is the wind velocity. These equations collectively describe how the power coefficient C_p varies as the turbine operates. By controlling λ and β , designers can estimate where the turbine runs best and use that information to improve control strategy and efficiency (Hannan et al., 2023; Stadtherr, 2019).

4.4 Simulink model of the wind turbine

Simulink is widely used to model and test how a wind-turbine system behaves before building it in hardware. It lets engineers connect the turbine, generator, and converter blocks into one working setup and watch how they react to changes in wind speed or load.

In this work, Figure 2 shows how all of these parts fit together in one model so that the complete system can be run and studied in real time (Hannan et al., 2023).

4.5 Simulink model of the power coefficient

Figure 3 illustrates the subsystem of the wind turbine model responsible for calculating the power coefficient C_p . The inputs, namely, the tip-speed ratio (λ) and the blade-pitch angle (β), are fed into the block implementing the mathematical relation for $C_p(\lambda, \beta)$. This subsystem plays a crucial role in achieving precise control over the aerodynamic characteristics of the turbine, thereby optimizing its efficiency across varying wind and operational conditions (Stadtherr, 2019). The wind turbine parameter values are shown in Table 1.

4.6 PMSG electrical model

The stator voltage equations in the rotating dq reference frame are given by Equations 5, 6:

$$v_d = R_s i_d + L_d \frac{di_d}{dt} - \omega_e L_q i_q \quad (5)$$

$$v_q = R_s i_q + L_q \frac{di_q}{dt} + \omega_e (L_d i_d + \psi_f) \quad (6)$$

where:

v_d, v_q : dq -axis stator voltages (V)

i_d, i_q : dq -axis stator currents (A)

R_s : stator resistance. (Ω)

L_d, L_q : stator inductances (H)

ψ_f : permanent magnet flux linkage (Wb)

$\omega_e = p\omega$: electrical angular speed (rad/s),

p being the pole-pair number.

Electromagnetic torque:

The electromagnetic torque produced by the machine is expressed by Equation 7:

$$T_e = \frac{3}{2} p (\psi_f i_q + (L_d - L_q) i_d i_q) \quad (7)$$

Mechanical dynamics:

The mechanical dynamics of the turbine-generator system are governed by Equation 8:

$$J \frac{d\omega_t}{dt} = T_t - T_e - B\omega_t \quad (8)$$

where J is the rotor inertia and B is the viscous friction coefficient.

4.7 Rectifier and DC-Link

The three-phase diode bridge rectifies the generator output. The average DC-link voltage is given by Equation 9:

$$V_{dc,avg} = \frac{3\sqrt{2}}{\pi} V_{LL} - 2V_d \quad (9)$$

where $V_d \approx 0.7$ V is the forward voltage drop of each diode.

The DC-link voltage ripple is mitigated using a capacitor C_{dc} which is sized according to Equation 10:

$$C_{dc} \geq \frac{I_{dc}}{6f_r \Delta V_{dc}} \quad (10)$$

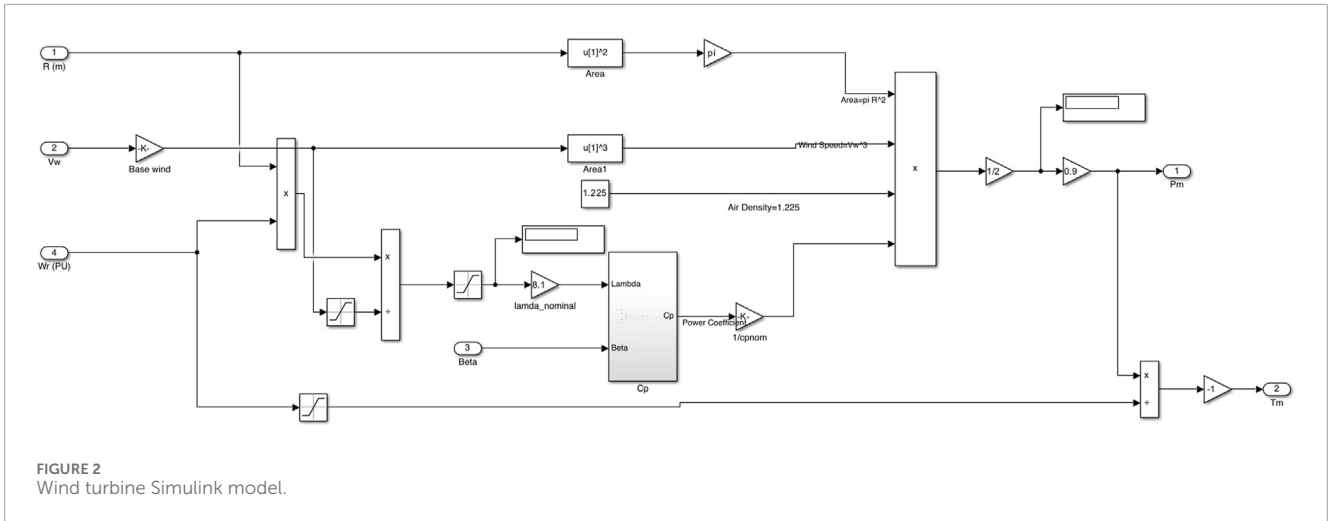


FIGURE 2 Wind turbine Simulink model.

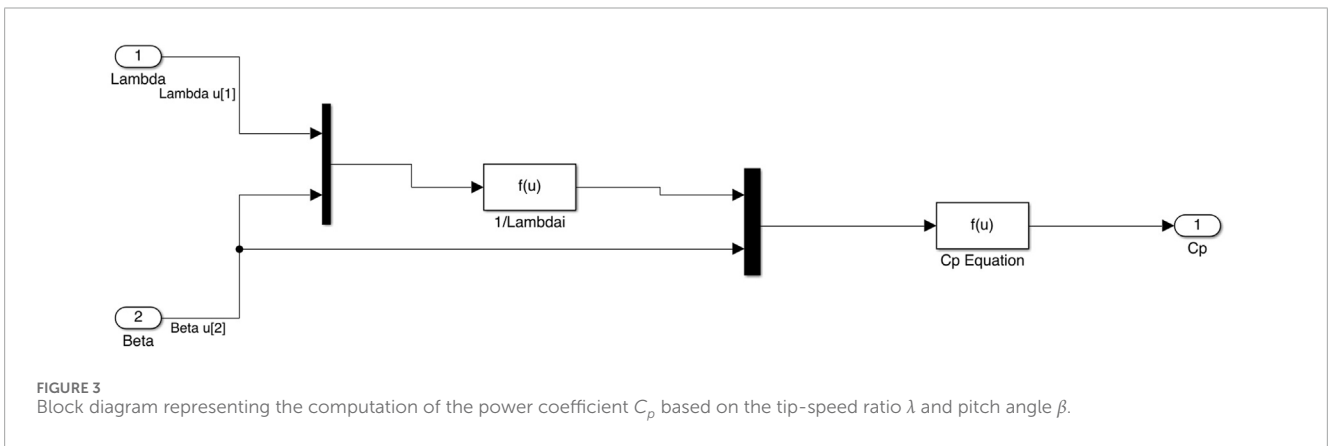


FIGURE 3 Block diagram representing the computation of the power coefficient C_p based on the tip-speed ratio λ and pitch angle β .

TABLE 1 Simulation wind turbine parameters.

Wind turbine parameters	Value and unit
Radius	1.03 m
Air density	1.22 kg/m ³
Wind velocity	8–12 m/s
β (pitch angle)	0
Theoretical power (P_{opt})	1692 W

where f_r is the rectified ripple frequency ($6 \times$ mechanical frequency).

4.8 SEPIC converter design

The SEPIC converter offers both step-up and step-down functionality while maintaining non-inverting polarity (Alsumiri and Althomali, 2017). Its topology is shown in Figure 4. In a SEPIC-based WECS, the rectified generator output is first fed to

the converter input, where the two inductors and coupling capacitor regulate energy transfer between the input and output stages. During the MOSFET's ON period, energy is stored in both inductors, while in the OFF period, this energy is released through the diode to the load or DC link, ensuring continuous input current and low ripple at the output. The control loop typically governed by a MPPT algorithm adjusts the duty cycle of the MOSFET to maintain operation at the generator's optimal power coefficient. The converter keeps changing its duty cycle when the wind or the load shifts. By doing this, it pulls as much energy as possible from the turbine and still holds the DC-bus voltage steady. When combined with intelligent controllers such as FLC, PSO, or hybrid learning models, the SEPIC converter topology provides a robust platform for achieving fast, stable, and efficient power regulation under real-world disturbances.

4.8.1 Operating modes

Two operating states exist:

Mode I (Switch ON): Inductors L_1 and L_2 store energy from the input source, while capacitor C_1 charges through L_3 if coupled.

Mode II (Switch OFF): Inductor currents discharge through diode D to the output, while C_1 transfers its stored energy to C_{out} and the load.

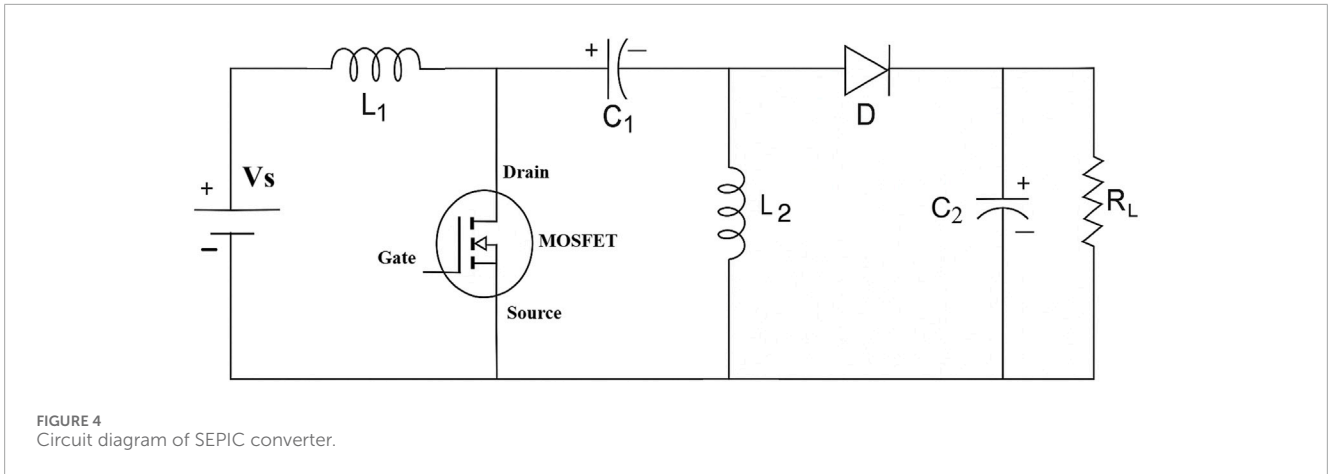


FIGURE 4
Circuit diagram of SEPIC converter.

4.8.2 Voltage gain

Applying inductor volt-second balance for continuous conduction mode, the voltage gain of the SEPIC converter is given by Equation 11:

$$\frac{V_o}{V_{in}} = \frac{(2 + D)(1 + D)}{(1 - D)} \quad (11)$$

At $D = 0.5$, $\frac{V_o}{V_{in}} = 7.5$; thus a 240 V input yields approximately 1800 V theoretical maximum, but practical design limits the output to 600 V.

4.8.3 Duty cycle range

Considering the effect of the diode forward voltage drop V_d , the duty cycle of the SEPIC converter can be expressed as Equation 12:

$$D = \frac{V_o + V_d}{V_o + V_d + V_{in}} \quad (12)$$

Hence, $D_{max} = 0.714$ at $V_{in,min} = 240\text{V}$ and $D_{min} = 0.667$ at $V_{in,max} = 300\text{V}$.

4.8.4 Inductor design

To limit the peak-to-peak inductor current ripple to 1% of the input current I_{in} the inductances L_1 and L_2 are calculated using Equation 13:

$$L_1 = L_2 = \frac{V_{in,min} D_{max}}{\Delta I_L f_{sw}} \quad (13)$$

Substituting the design values $V_{in,min} = 240\text{V}$, $D_{max} = 0.714$, $\Delta I_L = 0.01 I_{in} = 0.088\text{A}$, and $f_{sw} = 10\text{kHz}$, the inductances are obtained as shown in Equation 14:

$$L_1 = L_2 \approx 1.95 \times 10^{-1}\text{H} \quad (14)$$

4.8.5 Coupling capacitor C_1

To limit the peak-to-peak output voltage ripple to 1% of V_o the output capacitor C_1 is calculated using Equation 15:

$$C_1 = \frac{I_{out} D_{max}}{\Delta V_C f_{sw}} \quad (15)$$

Assuming $I_{out} = 3.5\text{A}$ and $\Delta V_{C1} = 6\text{V}$, we obtain $C_1 \approx 4.17 \times 10^{-5}\text{F}$.

4.8.6 Output capacitor C_{out}

To limit the output voltage ripple, the output capacitor is calculated using Equation 16:

$$C_{out} = \frac{I_{out} D_{max}}{0.5 \Delta V_{out} f_{sw}} \quad (16)$$

Substituting the design values yields $C_{out} = 8.33 \times 10^{-5}\text{F}$.

The maximum ESR is limited to maintain voltage ripple within specifications, given by Equation 17:

$$ESR_{max} = \frac{0.5 \Delta V_{out}}{I_{L1,peak} + I_{L2,peak}} \approx 0.243\Omega \quad (17)$$

4.8.7 Input capacitor

To smooth the input current, the RMS value of the input capacitor current is calculated using Equation 18:

$$I_{cin,rms} = \frac{\Delta I_L}{\sqrt{12}} = 0.025\text{A} \quad (18)$$

A 100 μF electrolytic capacitor rated above 400 V satisfies this requirement. The SEPIC converter design values are summarized in Table 2.

The tracking efficiency is defined as the ratio between the actual energy captured by the MPPT controller and the theoretical maximum extractable energy under identical wind conditions over the same time horizon, as given in Equation 19:

$$\eta_{track}(\%) = \frac{\int_0^T P_{MPPT}(t) dt}{\int_0^T P_{opt}(t) dt} \times 100 \quad (19)$$

where $P_{MPPT}(t)$ represents the instantaneous power obtained using the proposed Hybrid AOO-based MPPT, and $P_{opt}(t)$ denotes the reference maximum power computed from the turbine's optimal power-speed characteristic.

The SEPIC converter design presented in Table 2 was based primarily on ideal component assumptions, which is standard practice during the preliminary analytical sizing of inductors, capacitors, and switching elements (Hussain and Mishra, 2014). Conduction and switching losses, ESR-related ripple effects, and

TABLE 2 Designed SEPIC converter values.

Parameter	Value/Unit
Input voltage (V_{in})	240–300 V
Output voltage (V_o)	600 V
Duty cycle (D)	$D_{min} = 0.667, D_{max} = 0.714$
Switching frequency (f_{sw})	10 kHz
Inductors (L_1, L_2)	0.195 H each
Coupling capacitor (C_1)	0.0000417 F
Output capacitor (C_{out})	0.0000833 F
Output current (I_{out})	3.5 A
Input capacitor (C_{in})	100 μ F/400 V
Maximum ESR (ESR_{max})	0.243 Ω
Inductor ripple (ΔI_L)	0.088 A
Capacitor ripple (ΔV_{C1})	6 V

diode voltage drops were not explicitly included in the initial closed-form calculations; however, these non-ideals were incorporated in the MATLAB/Simulink simulation model, where parasitic resistances, switching behaviour, and ESR values were added to more accurately reflect practical operating conditions [Borni et al. \(2021\)](#). This two-stage approach, ideal analytical design followed by non-ideal simulation validation, is widely adopted in converter-based WECS studies.

5 Methodology

The [Figure 5](#) shown the wind Turbine Simulink model, and the control layer of the proposed WECS governs the SEPIC converter to ensure the captured turbine power is always maximized. The MPPT block measures the DC-link voltage V_{dc} and current I_{dc} .

At each sampling instant, the instantaneous output power is calculated using [Equation 20](#):

$$P = V_{dc} \times I_{dc} \quad (20)$$

The duty ratio acts as the control command for the SEPIC converter and is constrained within the allowable operating range as defined in [Equation 21](#):

$$D \in [D_{min}, D_{max}] \quad (21)$$

MPPT strategies compared: (i) P&O, (ii) FLC, (iii) PSO, and (iv) the proposed Hybrid AOO. All methods share identical, sampling time, wind profile, and SEPIC ([Vendoti et al., 2025](#); [Alsumiri and Althomali, 2017](#)).

5.1 MPPT design using P&O method

MPPT is a technique used in renewable energy systems, particularly in wind energy systems, to maximise the energy extracted from the energy source ([Eldodor et al., 2020](#)). The fundamental objective of MPPT is to ensure that the system operates at its most efficient point, where the power output is maximised. In any renewable-energy setup, the power that comes out depends on nature itself. Wind speed goes up and down all day, so the working point of the system cannot stay fixed. It must move with the wind if we want the best output. That is what MPPT does. It's the controller's way of finding the sweet spot where the turbine gives the maximum power. The efficiency of the energy conversion component is fundamental to the importance of the MPPT device. Problematic efficiency occurs due to the inability to follow the MPP. When the system accurately follows the MPP, the efficiency is maintained at a high value; however, failure to do so will lead to a drop in efficiency and increased overall generation costs. The P&O approach is probably the most common. People like it because it's simple and cheap to build. The controller nudges the voltage or current a little, watches what happens to the output power, and keeps moving in the direction that makes power rise. If the power drops, it changes direction. Step by step, the operating point stays close to where the turbine delivers the most energy.

This iterative approach helps the system track the maximum power point, even as environmental conditions change. The P&O method is considered one of the best MPPT techniques due to its simplicity and efficiency. It requires minimal computational resources and can be easily implemented in microcontrollers, making it a cost-effective solution for many renewable energy systems. Additionally, the P&O method does not require detailed knowledge of the system's characteristics, unlike the INC technique, which may require more complex calculations. Although the P&O method may have limitations in rapidly changing environmental conditions, its ease of use and reliable performance in steady-state conditions make it a preferred choice for many practical applications in wind energy systems. P&O technique iteratively perturbs the duty cycle and observes power change.

1. At the k -th sampling instant, the voltage $V(k)$ and current $I(k)$ are measured, and the instantaneous power is computed using [Equation 22](#):

$$P(k) = V(k) \times I(k). \quad (22)$$

2. Compute the power difference $\Delta P = P(k) - P(k-1)$ and the voltage difference $\Delta V = V(k) - V(k-1)$.
3. Update the duty cycle according to

$$D(k+1) = \begin{cases} D(k) + \Delta D, & \text{if } \Delta P > 0 \text{ and } \Delta V > 0, \\ D(k) - \Delta D, & \text{if } \Delta P < 0 \text{ and } \Delta V > 0, \\ D(k) - \Delta D, & \text{if } \Delta P > 0 \text{ and } \Delta V < 0, \\ D(k) + \Delta D, & \text{if } \Delta P < 0 \text{ and } \Delta V < 0. \end{cases}$$

4. Apply the new duty cycle and repeat.

The perturbation step ΔD is typically chosen within the range of 0.001–0.01. Smaller step sizes reduce output ripple but slow down convergence, while larger step sizes accelerate convergence at the expense of increased oscillations around the maximum

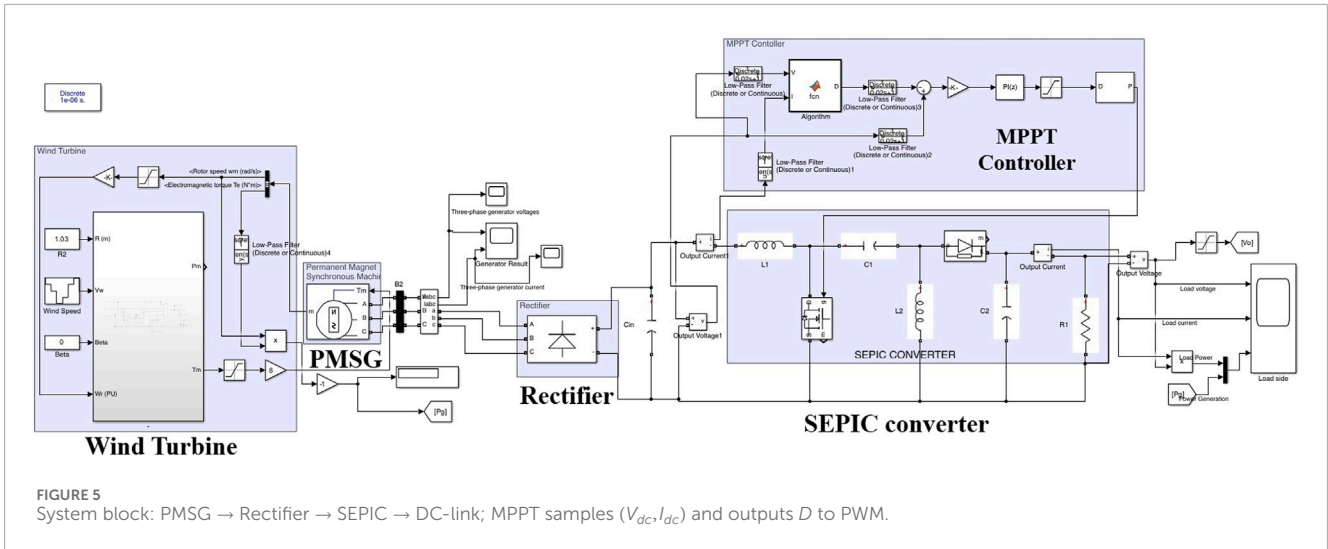


FIGURE 5 System block: PMSG → Rectifier → SEPIC → DC-link; MPPT samples (V_{dc}, I_{dc}) and outputs D to PWM.

power point. Pseudocode of P&O explains the control logic of the conventional P&O MPPT algorithm, commonly implemented in small-scale WECS employing PMSGs. The algorithm operates by periodically sampling the DC-link voltage and current to compute the instantaneous power and then determining the variations in power (ΔP) and voltage (ΔV) between consecutive samples. Based on these deltas, it adjusts the duty cycle (D) of the DC-DC converter: if $\Delta P > 0$, the previous perturbation was in the correct direction, and the duty cycle is updated in the same direction; otherwise, the direction is reversed to ensure tracking toward the maximum power point. The logic also considers the sign of ΔV to fine-tune how the duty ratio is modified, helping the boost converter maintain both voltage and current near their optimal operating points.

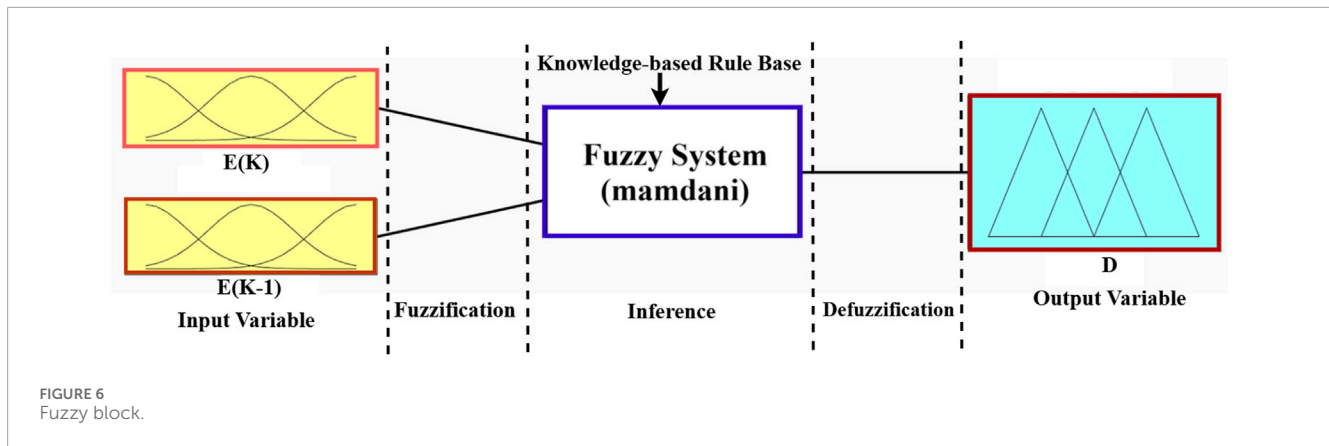
Pseudocode of Perturb and Observe (P&O) MPPT.

- 1. Start**
Define Constants:
Upper and lower voltage limits: $V_{max} = 300, V_{min} = 240$
Initial voltage: $V_{in} = 270$
Perturbation step size: $\Delta D = 0.00005$
- 2. Initialize Persistent State Variables:**
first run $V_{old} = 0, P_{old} = 0, D_{old} = D_{in}$
- 3. Compute Present Values:**
Instantaneous power: $P = V \times I$
Differences: $\Delta P = P - P_{old}, \Delta V = V - V_{old}$
- 4. Decision Based on Power Change:**
 $\Delta P = 0 \Rightarrow D = D_{old}$ (No change in power)
 $\Delta P > 0, \Delta V > 0 \Rightarrow D = D_{old} - \Delta D$ (Left of MPP: reduce duty to raise V)
 $\Delta P > 0, \Delta V < 0 \Rightarrow D = D_{old} + \Delta D$ (Right of MPP: increase duty to lower V)
 $\Delta P < 0, \Delta V > 0 \Rightarrow D = D_{old} + \Delta D$ (Reverse previous direction)
 $\Delta P < 0, \Delta V < 0 \Rightarrow D = D_{old} - \Delta D$
- 5. Saturation Check:**
If $D > D_{max}$ or $D < D_{min}$, then $D = D_{old}$
- 6. Update Memory:**
 $V_{old} = V, P_{old} = P, D_{old} = D$

Because this MPPT scheme relies solely on electrical quantities, it eliminates the need for any wind-speed sensor, making it highly suitable for small, low-cost, or standalone wind turbine installations. Although the standard P&O algorithm is robust and simple to implement, it exhibits certain limitations: under rapidly changing wind conditions, the output power often oscillates around the maximum point, reducing conversion efficiency. To mitigate these issues, researchers have proposed various adaptive and hybrid control techniques that enable faster convergence with minimal overshoot (Eldodor et al., 2020; Teklehaimanot et al., 2024). The aim is to bring the neat mathematical design of MPPT algorithms closer to what actually works once converter limits and fast wind changes come into play.

5.2 MPPT design using fuzzy logic controller (FLC) algorithm

MPPT using the FLC is an advanced intelligent control strategy that mimics human decision-making to manage system nonlinearities and parameter uncertainties in WECS. There are several ways to implement MPPT. Each method is effective in some cases, though none are a perfect solution. The FLC does not rely on perturbations of electrical variables, as with conventional numerical techniques such as P&O. Instead, the FL controller applies linguistic reasoning and heuristic rules to identify the proper degree of duty cycle change the DC-DC converter should exhibit. This approach eliminates the need for an explicit mathematical model of the turbine generator system, making it particularly advantageous for variable-speed wind applications where system parameters change dynamically (Borni et al., 2021; Lopez-Flores et al., 2024). In the proposed WECS, the Fuzzy Logic MPPT controller regulates the duty cycle of a SEPIC converter connected to a PMSG. The control loop begins with the acquisition of the DC-link voltage (V) and current (I), which are filtered using low-pass filters to eliminate high-frequency noise. The instantaneous power is then computed as $P = V \times I$, followed by the derivation of two primary control inputs: the error, defined as $E = \frac{dP}{dV}$, and the change in error, given by $\Delta E = E(k) -$



$E(k-1)$. These inputs represent the slope of the power–voltage curve and its rate of change, serving as indicators of whether the operating point lies to the left or right of the maximum power point (Vendoti et al., 2025). The trend-based input variables are defined in Equation 23:

$$E(k) \approx \frac{\Delta P}{\Delta V} = \frac{P(k) - P(k-1)}{V(k) - V(k-1)}, \quad \Delta E(k) = E(k) - E(k-1) \quad (23)$$

Inference: Seven triangular membership functions (MFs) are defined for each variable {NB, NM, NS, Z, PS, PM, PB}. A Mamdani type inference mechanism with max–min composition and centroid defuzzification is employed to compute the change in duty cycle (ΔD) as expressed in Equation 24:

$$\Delta D = \frac{\sum_i \mu_i^{(out)} D_i}{\sum_i \mu_i^{(out)}} \quad (24)$$

The updated duty ratio at the next sampling instant is then obtained using Equation 25:

$$D(k+1) = D(k) + \Delta D \quad (25)$$

Figure 6 illustrates the structure and functional components of the proposed fuzzy logic controller. Figure 7 The fuzzy inference system (FIS) utilizes two inputs, such as input error (E) and change in error (ΔE) to determine the output, the incremental duty-cycle adjustment (ΔD). The inference mechanism operates using a set of linguistic rules and membership functions (MFs), where each input and output variable is divided into seven fuzzy subsets: Negative Big (NB), Negative Medium (NM), Negative Small (NS), Zero (Z), Positive Small (PS), Positive Medium (PM), and Positive Big (PB). The controller uses triangular MFs placed symmetrically around the zero point to provide higher resolution near the maximum power region. The fuzzy-rule base defines how the input variables interact to produce the control output, The Mamdani inference method with max–min composition and centroid defuzzification is applied to yield smooth duty-cycle changes. The updated duty ratio is calculated as expressed in Equation 26:

$$D(n) = D(n-1) + \Delta D \quad (26)$$

This ensures that the converter continuously tracks the maximum power point in real time.

Pseudocode of the Fuzzy Logic MPPT algorithm.

1. Start:

Inputs: current (I) and voltage (V).

2. Compute Instantaneous Power

Multiply filtered inputs to obtain: $P = V_f \times I_f$

Store the previous sample using a memory/delay block.

3. Compute Incremental Changes

Power change: $\Delta P = P - P_{old}$

Voltage change: $\Delta V = V_f - V_{f,old}$

4. Calculate Instantaneous Error and Error Change

Compute instantaneous slope (error): $E_k = \frac{P}{V_{if}}$

Previous error E_{k-1} is stored in a memory block.

Compute change in error: $\Delta E_k = E_k - E_{k-1}$

5. Decision Stage (Fuzzy Logic Control)

Inputs to the fuzzy controller: Error (E_k) and Change in error (ΔE_k).

The fuzzy inference system (FIS) determines the duty-cycle adjustment (ΔD)

based on the defined membership functions (e.g., Negative Big, Zero, Positive Small).

The fuzzy rule base interprets the slope direction and trend to decide

whether to increase or decrease the duty cycle.

6. Update Duty Cycle

The final duty command is: $D = D_{old} + \Delta D$

This duty cycle is applied to the DC–DC (SEPIC) converter for control.

7. Feedback and Memory Update

Store the latest values for the next iteration: $P_{old} = P$,

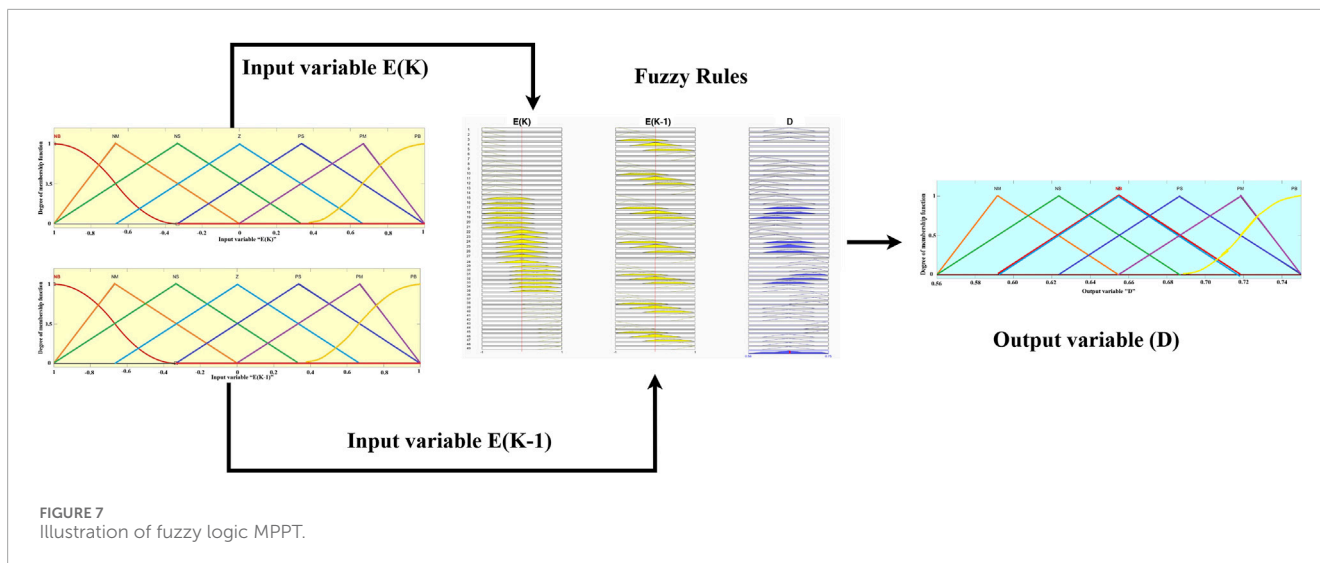
$V_{f,old} = V_f$, $E_{k-1} = E_k$, $D_{old} = D$

The updated duty cycle keeps the wind system close to its maximum power point.

8. End of Loop Continuation

The system continuously iterates through the above steps to track the MPP in real time.

Pseudocode of FLC explains the repeating steps of the control loop: signal measurement, fuzzy decision-making, and the duty-cycle update. The loop starts with conditioning the voltage and current signals, then calculates the instantaneous power and its error terms. Once the fuzzy rules are applied, the converter adjusts



almost instantly, reaching the maximum-power point with little or no oscillation.

Table 3 lists the fuzzy rule base used in the controller (Sarathi and Rama Prabha, 2025). The rules link the two inputs, such as input error (E) and change in error (ΔE) to the duty-cycle adjustment (D). These linguistic rules instruct the controller how to respond to different combinations of E and ΔE . For instance, if both E and ΔE are positive, the duty cycle is reduced to bring the operating point back toward the maximum-power region. Conversely, when both are negative, the controller increases the duty cycle to capture more energy. By applying these fuzzy logic rules, nonlinear mapping is created between the input pair ($E, \Delta E$) and the output ΔD , allowing the controller to adapt dynamically without requiring a detailed system model (Borni et al., 2021).

The fuzzy logic based MPPT method is not only simple, but it also responds well when wind input changes rapidly (Lopez-Flores et al., 2024; Vendoti et al., 2025). The fuzzy controller, based on trends instead of instantaneous derivative calculations, performs better than many conventional schemes with given noise conditions, and slow sensors (Pande et al., 2021). The fuzzy MPPT controller, when used with a SEPIC converter, also maintains continuous current and minimizes electromagnetic noise. With these together the conversion efficiency will increase and the reliability of the system will improve. In summary, fuzzy-logic MPPT affords a flexible and self-adaptive method to regulate a SEPIC converter based system for wind applications. Fuzzy-logic MPPT utilizes both rules, based reasoning and numerical accuracy, therefore the MPPT algorithm will continue to perform well regardless of fast changes in wind speed. The simplicity of combining linguistic rules, adaptive membership functions, and real-time inference technology has made fuzzy control, the most-faithful intelligent MPPT method available today (Lopez-Flores et al., 2024; Vendoti et al., 2025).

5.3 MPPT design using PSO algorithm

The PSO algorithm simulates the social behavior of birds searching for food (Kennedy and Eberhart, 2021). In the proposed

TABLE 3 Rules table for fuzzy inference system.

Output D	Input e						
	Input Δe	NB	NM	NS	Z	PS	PM
NB	Z	Z	NS	NM	NB	NB	NB
NM	Z	NS	NS	NM	NM	NB	NB
NS	Z	Z	NS	NS	NM	NM	NB
Z	Z	Z	Z	Z	Z	Z	Z
PS	PS	PS	Z	Z	Z	Z	Z
PM	PM	PS	PS	Z	Z	Z	Z
PB	PB	PM	PS	PS	Z	Z	Z

SEPIC converter-based WECS, PSO treats the converter duty ratio command as the variable to be optimized by a “swarm” of particles. Each particle represents an operating point, and its fitness value is evaluated as the generated power, computed from the DC-link voltage and current as $P = V \times I$.

At each iteration, all particles update their velocity and position based on two learned components: the best value found by the particle itself ($pbest$) and the best-found value among all particles in the swarm ($gbest$) (Kennedy and Eberhart, 2021; Ala et al., 2023). This process alternates between exploration (searching for new operating points) and exploitation (refining the most promising points), thereby achieving an effective balance between global search and local refinement without requiring detailed turbine modeling. This property makes PSO particularly advantageous for nonlinear and time-varying systems where parameters drift over time, as it does not depend on explicit aerodynamic equations. Consequently, PSO is widely recognized in literature (Eswaraiah

and Balakrishna, 2024; Pande et al., 2024). as a strong, model-free alternative to conventional hill-climb and P&O algorithms.

In our system, PSO optimizes only one variable the duty ratio (D) of the SEPIC converter. The PSO implementation in this work employed a swarm of four particles, and this choice is justified based on both WECS-specific literature and real-time control requirements. Unlike high-dimensional optimization problems, MPPT in wind energy systems is fundamentally a single-variable optimization task, where only the converter duty ratio is being optimized. Prior studies have shown that for such low-dimensional search spaces, using large swarms (10–20 particles) provides no additional benefit in convergence accuracy while substantially increasing computational burden. Several researchers, including (Ala et al., 2023; Arabi et al., 2024; Pande et al., 2021), have demonstrated that three to five particles are sufficient to achieve fast and stable MPPT convergence in WECS applications. Furthermore, MPPT algorithms must operate within tight real-time constraints imposed by converter switching frequencies and embedded microcontroller execution times. Increasing the swarm size directly increases the computation per switching cycle, which can delay duty-cycle updates and degrade performance during rapid wind speed variations. To maintain fairness and consistency in comparison, we also adopted a four-candidate structure for the Hybrid AOO algorithm and therefore selected the same number of candidates for PSO to ensure equal computational effort per control interval. Our sensitivity analysis further validated this choice: swarm sizes of 2, 4, 6, 10, and 20 particles were tested, and the configuration with four particles achieved the best balance of fast settling time, low ripple, and stable convergence, while larger swarms increased computation time without improving tracking performance. For these reasons, the use of four particles in PSO is both literature-supported and performance-optimal for real-time WECS MPPT applications.

Pseudocode of the PSO-based MPPT.

1. Start

Inputs: current (I) and voltage (V).

2. Initialise

If empty, set: $u = 0$, counter = 0, $d_{\text{current}} = 0.9$, $g_{\text{best}} = 0.9$, $p = \text{zeros}(4, 1)$, $pb_{\text{best}} = \text{zeros}(4, 1)$, $v = \text{zeros}(4, 1)$, $dc = [250; 270; 280; 290]$.

3. Hold stage

Decision: counter ≥ 1 && counter < 300

Yes \rightarrow Output $D = d_{\text{current}}$, increment counter, Return.

No \rightarrow counter = 0, proceed.

4. Evaluate Current Candidate

Compute power: $P = V \times I$.

If current phase is a probe ($u \in \{1..4\}$) and $P > p(u)$

update personal slot best: $p(u) = P$; $pb_{\text{best}}(u) = d_{\text{current}}$.

5. Advance Phase Scheduler

$u = u + 1$; if $u = 6 \rightarrow u = 1$.

6. Phase Actions ($u = 1$ to 5)

$u = 1, 2, 3, 4$: Probe candidates

Set $D = dc(u)$ (candidate duty), $d_{\text{current}} = D$; counter = 1;

Return (enter hold stage).

$u = 5$: Selection + PSO Updates

Pick Global Best: $[m, j] = \max(p)$; $g_{\text{best}} = pb_{\text{best}}(j)$.

Output $D = g_{\text{best}}$; $d_{\text{current}} = D$; counter = 1.

Voltage Update (for each slot $k = 1$ to 4):

$$v(k) = \text{update}(v(k), pb_{\text{best}}(k), dc(k)),$$

g_{best} with const $w = 0.1$, $c_1 = 1.2$, $c_2 = 1.2$.

Duty Cycle Update (for each slot $k = 1$ to 4):

$$dc(k) = \text{updateduty}(dc(k), v(k)) \rightarrow \text{clamps to } [240, 300].$$

7. Return (enter hold stage).

In this Pseudocode implementation, the PSO MPPT controller takes the inputs are voltage (V) and current (I) at every switching cycle to compute instantaneous power ($P = V \times I$). It maintains arrays for particle fitness (p), velocity (v), personal best (pb_{best}), and global best (g_{best}) across a small swarm of four particles. A short dwell time of approximately 300 switching intervals allows each candidate to operate long enough for accurate power evaluation. After testing all four candidates, the controller updates the command variables according to the standard PSO velocity–position update rule, where the inertia weight is $w = 0.1$ and the cognitive and social learning coefficients are $C_1 = C_2 = 1.2$.

The commanded duty ratio (D) is then computed and constrained within the converter limits of 240–300 units. This optimization process runs continuously during each switching interval, without the need for explicit system dynamics or turbine parameters, relying solely on the electrical measurements affected by natural wind variations. Once the four candidates have been evaluated, the procedure repeats cyclically for continuous real-time tracking. This coding pattern mirrors the standard PSO recurrence while being tailored to real-time power electronics: (i) a very small swarm reduces computational overhead; (ii) fitness as direct electrical power eliminates wind sensors and turbine models; (iii) bounded updates guarantee converter safety; and (iv) a short evaluation dwell improves signal-to-noise ratio in power measurements. Reported WECS studies consistently find PSO MPPT to converge faster and with less steady-state oscillation than basic P&O, particularly when embedded in intelligent or hybrid controllers (e.g., PSO-tuned PI/FLC) (Borni et al., 2021; Arabi et al., 2024). PSO's main trade-off is that poorly tuned inertia or gains can induce premature convergence or overshoot under rapidly varying winds; however, modest parameter values, small swarms, and bounded step sizes as used in the code generally yield stable, fast tracking suitable for low-cost DSP or MCU deployment (Pande et al., 2021; Ala et al., 2023).

Each particle represents a candidate converter duty ratio. The swarm updates its position using its own best experience (pb_{best}) and the group's best experience (g_{best}).

Velocity update:

The velocity of each particle is updated according to Equation 27:

$$v_i(t+1) = wv_i(t) + c_1r_1[pb_{\text{best}_i} - x_i(t)] + c_2r_2[g_{\text{best}} - x_i(t)] \quad (27)$$

Position update:

The position of each particle is updated according to Equation 28:

$$x_i(t+1) = x_i(t) + v_i(t+1) \quad (28)$$

where:

w inertia weight ($0 \leq w \leq 1$)

c_1, c_2 — acceleration coefficients.

r_1, r_2 — uniform random numbers (0–1)

The fitness of each particle is evaluated as the instantaneous converter power, as expressed in Equation 29:

$$f_i = P_i = V_i \times I_i \quad (29)$$

5.4 Proposed MPPT design using hybrid animated oat optimization (AOO)

The Hybrid AOO based MPPT technique is a bio-inspired metaheuristic modelled on the hygroscopic curling/rolling and projectile seed-spreading behavior of *Avena sativa* (oat) grains during germination and dispersion. In a WECS context, this physical analogy is adapted into a voltage-based search that steers the DC - DC stage toward the maximum power point (MPP) without requiring a turbine model, similar in spirit to other nature-inspired MPPT approaches that balance exploration and exploitation to overcome local maxima (Arabi et al., 2024; AboRas et al., 2025; Pande et al., 2021). Consistent with intelligent WECS implementations that combine MPPT and converter design (often SEPIC) for robustness and fast dynamics (Vendoti et al., 2025), AOO uses measured DC-link voltage and current only, keeping sensing minimal while preserving adaptability. In practice, the controller tests a small group of four possible operating voltages one after another. Each voltage is held for about 75 switching periods so the converter output can settle before the next one is checked. This short “dwell time” helps average out the switching noise and makes comparison between candidates fairer under real converter dynamics.

Each candidate is a potential reference voltage V_{MPP} , constrained within a bounded range (e.g., 280–300 V for SEPIC operating conditions), and its fitness is defined as the instantaneous power $P = V \times I$. The algorithm maintains a persistent swarm-state memory p , the candidate array dc , the best-so-far voltage d_{best} , and an iteration counter to ensure that subsequent updates can leverage historical information while remaining adaptive to new data. To handle sudden wind transients, the AOO algorithm includes a fast reset mechanism that re-seeds all candidates around the currently measured voltage whenever a large power jump is detected (e.g., $\Delta P > 20$ W or $> 20\%$ of the previous power). Such resets are commonly recommended in metaheuristic-based WECS MPPT literature to prevent stagnation and to reduce recovery time after step disturbances (Arabi et al., 2024; AboRas et al., 2025; Pande et al., 2021).

During the update phase, AOO alternates between *exploration* and *exploitation*. In the exploration phase, candidates are randomly distributed around the mean position X_m and the best position X_b , modulated by a time-varying contraction factor: $c = 1 - \left(\frac{t}{T_{max}}\right)^3$, which gradually narrows the search radius as convergence progresses. In the exploitation phase, AOO refines the worst-performing candidate using two bio-inspired operators: (i) *hygroscopic rolling* (representing rotational creeping toward favorable conditions), and (ii) *ejection/projectile motion* (ballistic relocation for rapid convergence).

To prevent premature convergence, Hybrid AOO applies a small stochastic “diversity nudge” to the non-worst candidates

following each exploitation step. After every update, all candidates are clamped within the admissible voltage range, and the control output d_{best} is assigned as the reference voltage to the SEPIC converter. A mild forgetting factor (e.g., $p \leftarrow 0.9p$) discounts stale fitness data, ensuring that recent measurements dominate decision-making. This workflow mirrors the light weight, embedded-friendly designs used in WECS where computation and memory must be tightly bounded (Borni et al., 2021; Arabi et al., 2024). Empirically, AOO demonstrates rapid convergence, low steady-state ripple, and robust transient tracking under variable wind, outperforming conventional hill-climbing and matching or exceeding other intelligent MPPTs that employ adaptive exploration and exploitation policies (AboRas et al., 2025; Vu et al., 2022). In particular, the bounded 4- candidate evaluation, 75-step dwell, large-jump reset, and time-decaying contraction collectively shorten settling time after wind steps and suppress post-convergence oscillation behavior aligned with recent reports on intelligent MPPT coupled to high-gain SEPIC (Vendoti et al., 2025). Because Hybrid AOO requires only V,I measurements and enforces hard limits on commanded voltage, it integrates cleanly with SEPIC-based WECS while maintaining converter safety (Pande et al., 2021; Hussain and Mishra, 2014).

Hybrid AOO integrates: Exploration through random dispersal (seed-spreading), Exploitation through hygroscopic rolling toward optimal moisture zones, Adaptive re-seeding to avoid local minima.

5.4.1 Mathematical formulation

Each candidate duty ratio D_i represents an oat grain. The search space bounds are defined as $[D_{min} = 0.65, D_{max} = 0.75]$. The power fitness of each candidate is evaluated as $P_i = V_i I_i$.

Exploration (spreading):

The duty ratio of each agent during the exploration phase is updated according to Equation 30:

$$D_i^{new} = D_i + \alpha(t)(\text{rand}() - 0.5)(D_{best} - D_i) \quad (30)$$

where $\alpha(t) = \alpha_0(1 - t/T_{max})$ is the time-decaying contraction factor that controls the exploration range.

Exploitation (rolling/projectile motion on worst candidate D_w):

The duty ratio during the exploitation phase is updated according to Equation 31:

$$D_w^{new} = D_w + \beta \sin(\theta)(D_{best} - D_{mean}) + \gamma \text{Lévy}(\lambda) \quad (31)$$

where β and γ are learning gains (0.4–0.6), θ is a random direction angle, and Levy flight introduces random long jumps to enhance global search diversity. Adaptive reseeded is triggered when all duty ratio values are re-initialized around the current best solution D_{best} if the condition in Equation 32 is satisfied:

$$\left| \frac{P_{new} - P_{old}}{P_{old}} \right| > 0.2 \quad (32)$$

5.4.2 Hybridization strategy

To reduce computation, only four candidate voltages are evaluated per cycle, similar to PSO, but AOO introduces two motion operators per iteration Exploration phase (30), Exploitation phase (31). The optimization sequence alternates every $T_{hi} = 75$ switching steps. The candidate yielding the highest power output P_i becomes the new D_{best} for the subsequent control cycle (Wang et al., 2025).

Pseudocode of the Hybrid AOO (Animated Oat Optimisation)-based MPPT.

1. Start

2. Initialise

If end of ctr (empty): u , d_{current} , $p1$ to 4, dc (1–4), counter, $dcnt$, $invert$, $istar$, $lastJP$, $discover$.

Default candidates: $dc = \{257, 288, 259, 290\}$ (clamped to $\{V_{\text{min}} = 250, V_{\text{max}} = 300\}$).

Other inits: $holdCount = 75$, $resetThr = 200$, $seedSpan = 2$, $V_{\text{batt}} = 200$.

3. Hold stage

Decision: $counter \geq 1$ && $counter \neq holdCount$?

Yes \rightarrow Output $D = d_{\text{current}}$, increment counter, Return.

No \rightarrow counter = 0, proceed.

4. Measure Current Power

Compute $P = V \times I$.

If current phase $u \in \{1$ to 4 $\}$ and $P > p(u)$, update the slot fitness: $p(u) = P$.

5. Advance Phase Scheduler

$u = u + 1$; if $u = 6 \rightarrow u = 1$.

6. Large Power Jump Reset

Compute $\Delta P = P - lastJP$; $lastJP = P$.

Decision: if $\Delta P > resetThr$ and $\max(p) < lastJP$?

Yes \rightarrow Re-seed around the current V :

$$dc(1) = clamp(dc(1) + 1 \cdot seedSpan, V_{\text{min}}, V_{\text{max}})$$

$$dc(2) = clamp(dc(2) - 1 \cdot seedSpan, V_{\text{min}}, V_{\text{max}})$$

$$dc(3) = clamp(dc(3) + 1 \cdot seedSpan, V_{\text{min}}, V_{\text{max}})$$

$$dc(4) = clamp(dc(4) - 1 \cdot seedSpan, V_{\text{min}}, V_{\text{max}})$$

Other fitness $\rightarrow p = 0$, slightly rewind $iter = \max(iter - 10, 1)$, $discover = 0$.

No \rightarrow continue.

7. Phase Actions ($u = 1$ to 5)

$u = 1, 2, 3, 4$ (Exploit candidate slots)

Output candidate duty: $D = clamp(dc(u), V_{\text{min}}, V_{\text{max}})$,

$d_{\text{current}} = D$, counter = 1, Return (enter hold stage).

$u = 5$ (Selections + AOO updates)

1. Select Best/Worst

Compute best = $\arg \max p$, worst = $\arg \min p$.

2. Shrink Schedule

$shrink = (iter/T_{\text{max}})$ (monotonically decreases; floor at 0).

3. Decision: Exploration vs. Exploitation

Exploration ($\text{rand} > 0.5$)

Compute wander term $W = (dc(j) - dc(\text{rand} - 1))/V_{\text{max}}$.

Let $X = dc$ (best), $Y = dc$ (worst).

$$dc(j) = clamp(X + 0.1 \cdot (X - Y) + wander)$$

$$dc(k) = dc(k) + 0.05 \cdot wander \text{ (for other slots)}$$

Exploitation ($\text{rand} \leq 0.5$): Hypsocomic rolling (revert lost only)

Let $A = dc$ (best), $B = dc(j)$.

$$dc(j) = clamp(B + 0.2 \cdot (A - B))$$

If overshoot: shift slightly towards midpoint.

Branch (5% disc): Eject local projector (reset only worst)

$$dc(\text{worst}) = clamp(dc(\text{best}) + 0.1 \cdot (dc(\text{best}) - V_{\text{min}}), V_{\text{min}}, V_{\text{max}})$$

Branch (5% disc): Introduce ultra-small “jitter” hops

TABLE 4 Comparative characteristics of MPPT algorithms.

Feature	P&O	Fuzzy	PSO	Hybrid AOO
Computation	Low	Medium	Med-High	Medium
Response speed	Slow	Fast	Faster	Fastest
Steady-state ripple	High	Low	Low	Very low
Implementation	Easy	Moderate	Moderate	Moderate
Adaptability	Weak	Good	Good	Excellent

$$dc(j) = clamp(dc(j) + 0.01 \cdot randn())$$

Diverging edges:

$$dc(j) = clamp(dc(j) + 0.1 \cdot (rand() - 1) \cdot (V_{\text{max}} - V_{\text{min}}), V_{\text{min}}, V_{\text{max}})$$

4. Clamp $dc(j)$ into bounds

$$dc(j) = clamp(dc(j), V_{\text{min}}, V_{\text{max}}).$$

5. Output updated duty

Set new duty: $D = clamp(dc(j), V_{\text{min}}, V_{\text{max}})$;

$d_{\text{current}} = D$; Return.

6. Iter update

$iter = iter + 1$; if shrink triggered: $iter = 0.9 \cdot iter$.

8. Return

Keep last: $D = clamp(d_{\text{current}}, V_{\text{min}}, V_{\text{max}})$, set counter = 1.

Pseudocode of the hybrid AOO illustrates the complete operation cycle of the proposed AOO-based MPPT controller, which includes sequential evaluation of four candidate duty ratios with a 75-step dwell period. During each cycle, instantaneous power is computed, and a large-jump reset is triggered when a significant power variation is detected. The algorithm then proceeds with the update phase, which alternates between:

Exploration: mean/best-guided spreading controlled by the contraction coefficient $c(t)$, and.

Exploitation: hygroscopic rolling or projectile update applied to the worst-performing candidate.

Each iteration is followed by clamping of D within the permissible limits and a mild forgetting factor to preserve adaptability before the next control cycle begins. Table 4 compares the qualitative characteristics of the four MPPT algorithms implemented in the SEPIC-based WECS, emphasizing differences in computational complexity, convergence speed, steady-state ripple, and adaptability but a uniform sampling interval of $1e-4$ s (0.0001 s) was applied across the entire simulation environment. The conventional P&O algorithm exhibits the lowest computational load and simplest implementation, relying solely on voltage and current perturbations. However, it suffers from slow dynamic response and high steady-state ripple due to its fixed perturbation step size.

The FLC enhances convergence by applying heuristic rules to the power-voltage slope, achieving faster response and lower ripple at a moderate computational cost (Borni et al., 2021). The PSO method further improves performance by simultaneously evaluating multiple duty-ratio candidates through swarm intelligence. Although PSO often reaches the optimal point

TABLE 5 Comparative discussion highlighting the fundamental novelty of hybrid AOO based MPPT.

Aspect	Conventional MPPT (P&O)	Intelligent MPPT (FLC)	Metaheuristic MPPT (PSO)	Existing hybrid MPPT	Proposed hybrid AOO–MPPT
Core optimization principle	Local perturbation or predefined turbine characteristics	Rule-based or data-driven inference	Population-based stochastic search	Combination of two known algorithms	Behavior-driven animated oat dynamics with worst-candidate correction
Search update mechanism	Fixed step perturbation	Fixed or tuned rule updates	Velocity/position or trigonometric updates	Sequential or weighted updates	Worst-candidate-centric rolling/projectile update strategy
Exploration–exploitation control	Poor balance	Implicit via rules	Controlled by algorithm parameters	Mostly parameter dependent	Adaptive switching between rolling and ejection behaviors based on search state
Dependence on parameter tuning	Low	High (membership functions, rules)	Moderate to high	Very high	Low; behavior-guided update dominates over parameter sensitivity
Steady-state oscillation suppression	Poor	Moderate	Moderate	Moderate	Explicit dwell-time-aware update with micro-perturbation control
Premature convergence avoidance	Not addressed	Limited	Partially addressed	Partially addressed	Worst-solution correction with minimal diversity preservation
Computational burden	Very low	Low to moderate	Moderate to high	High	Low (small population, selective candidate updates)
Robustness to rapid wind variations	Poor	Moderate	Moderate	Moderate	High due to adaptive reseeding and dynamic candidate correction
Fundamental novelty	Established classical methods	Established intelligent control	Established stochastic optimization	Algorithm-level mixing	New bio-inspired animated oat behavior translated into MPPT logic
Suitability for real-time WECS	High	High	Limited	Limited	High (fast convergence with reduced oscillations)

faster, the multiple fitness evaluations and position updates per iteration result in a slightly higher computational requirement (Ala et al., 2023).

The presented approach of the AOO converges even faster and maintains very small ripples about its calculated output. The AOO utilizes an exploration and exploitation switch, which added adaptive contraction and reseeding periodically so that it can recover fast when the wind is changing too fast. Similar to an iteration of the PSO, the AOO is lightweight enough to run on a DSP or small microcontroller in real time using lookup tables (Ali and Ahmad, 2020; Vendoti et al., 2025). The importance of fair and consistent tuning across all benchmark algorithms. The tuning procedures for P&O, FLC, and PSO were carried out in accordance with established WECS MPPT literature and validated through structured sensitivity

analyses, as detailed. For P&O, the perturbation step $\Delta D = 0.00005$ was selected according to established WECS literature, where small perturbation amplitudes are shown to reduce steady-state ripple while maintaining adequate convergence (AboRas et al., 2025; Borni et al., 2021; Pande et al., 2021). The duty-cycle constraints follow SEPIC converter operational limits (Alsumiri and Althomali, 2017). For FLC, the membership functions, linguistic rules, and scaling gains were tuned iteratively to minimize ripple and accelerate transient response. This tuning approach is widely supported by prior FLC-based MPPT research, where membership function width and rule-base adjustments directly influence settling time and ripple performance (Borni et al., 2021; Lopez-Flores et al., 2024; Vendoti et al., 2025). The effectiveness of this tuning is evidenced by our simulation results shown in Table 7, where FLC reduced

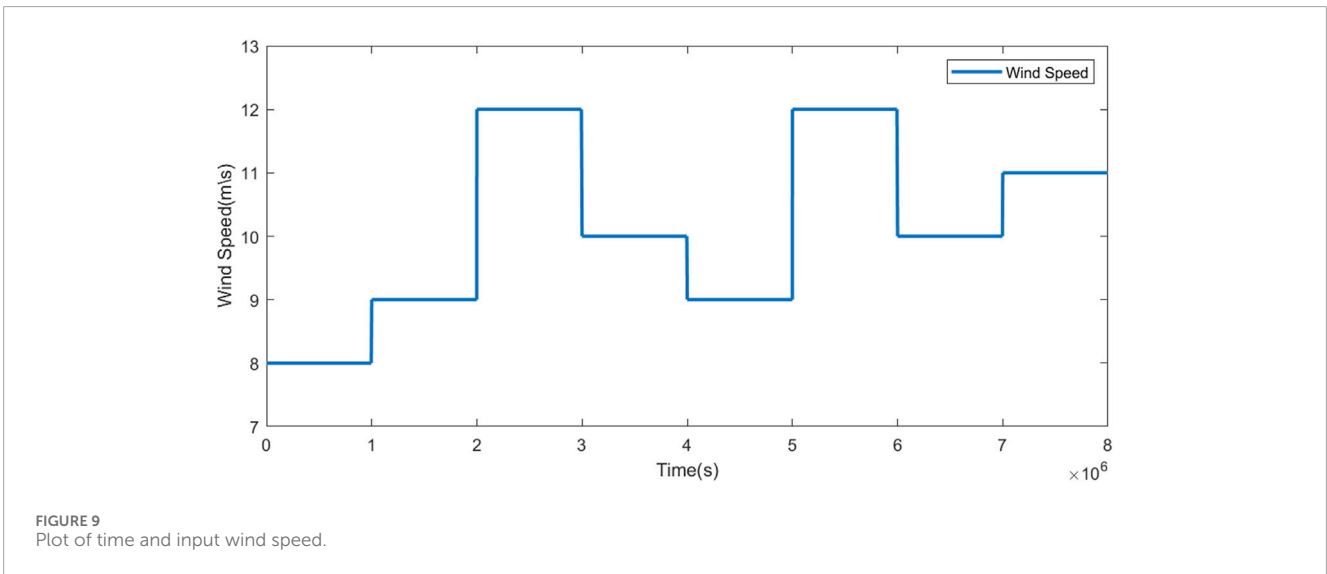
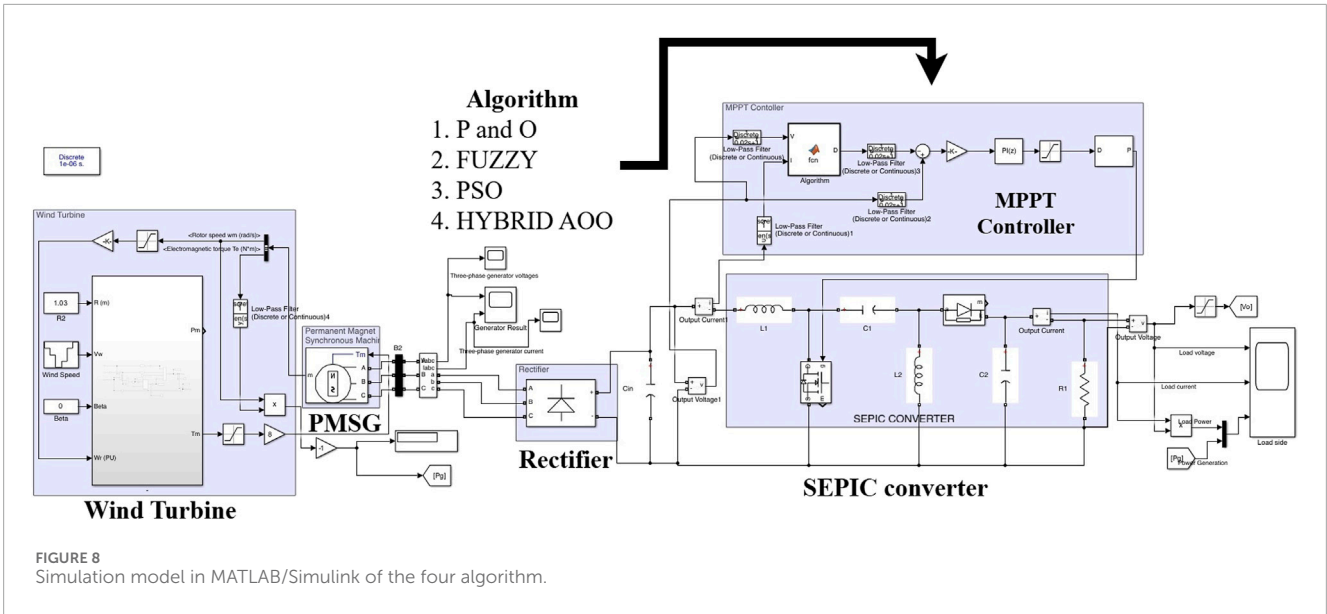


TABLE 6 Comparison of output power (in Watts) for different MPPT algorithms under varying wind speeds.

Wind speed (m/s)	P & O	Fuzzy	PSO	AOO (best)
8	581	601	600	619
9	775	810	804	834
10	993	1035	1030	1077
11	1236	1292	1290	1347
12	1502	1572	1569	1642

ripple to 25 W and settling time to 0.25 s. For PSO, the selected parameters (0.1, $c1 = c2 = 1.2$) align with WECS-specific PSO configurations reported in recent literature (Arabi et al., 2024; Pande et al., 2021).

The comparison of the algorithms is discussed in Table 5, which clearly distinguishes Hybrid AOO from conventional, Intelligent and metaheuristic MPPT methods, classical hybrid approaches, and parameter-tuned controllers. The table highlights the algorithmic-level innovations of Hybrid AOO, including: (i) The worst-candidate-centric update mechanism inspired by animated oat dynamics, (ii) Adaptive switching between rolling-based and projectile-based update strategies based on search conditions, (iii) Controlled micro-perturbation of remaining candidates to preserve

TABLE 7 Performance metrics of various MPPT controllers.

Parameter	P&O	PSO	Fuzzy	Hybrid AOO (best)
Average power (W)	1502	1569	1572	1642
Ripple (W)	70	38	25	15
Settling time (s)	0.50	0.30	0.25	0.12
Overshoot (%)	8.5	4.2	2.8	1.6
Tracking Eff. (%)	88.75	92.71	92.88	97.02

minimal diversity without increasing computational burden, and (iv) A dwell-time-aware update structure that explicitly suppresses steady-state oscillations while maintaining fast convergence. In conclusion, the general comparisons show quite substantially that while P&O is the easiest to build, AOO presents the better and more efficient solution when taking into account speed, stability and adaptability, and computation cost shown here for direct comparison for these different MPPT functions.

6 Results

This segment states a efficient and complete evaluation of the proposed control approaches. It is clarified that the developed small-scale WECS consists of a PMSG connected to a diode rectifier and a SEPIC converter. The SEPIC converter is governed by the respective MPPT controller, which adjusts the duty ratio to extract maximum power from the wind turbine. Four MPPT algorithms P&O, PSO, FLC, and the proposed Hybrid AOO were implemented and tested.

The Hybrid AOO MPPT decides the best operating voltage so the converter extracts maximum power at every wind speed, under identical operating conditions to evaluate system performance. The input wind velocity was varied between 8 m/s and 12 m/s, as shown in Figure 9, to examine the dynamic response of each control technique under fluctuating wind conditions. Each algorithm was individually applied to the SEPIC converter, and the system responses were recorded in terms of output voltage, current, power, tracking efficiency, and steady-state ripple. Subsequently, the controllers were compared comprehensively based on average power output, transient performance, overshoot behavior, and response time. The system and control parameters used for simulation are summarized in Table 1 and the comparative performance analysis results are provided in Tables 6, 7.

6.1 MATLAB/Simulink model configuration

This simulation models are complete WECS. The primary goal of this setup is to capture kinetic energy from the wind, convert it into electrical energy, and deliver it to a load with maximum efficiency. The one figures show four variations of the exact same system. The only difference between them is the specific algorithm used inside the “MPPT Controller” block. This indicates the purpose

of the simulation is to compare the performance of different MPPT algorithms: The detailed simulation environments for controller are shown in Figure 8. This includes all four algorithm, the conventional PandO structure, in which duty-cycle perturbations adjust the converter reference voltage until maximum power is detected and Fuzzy system includes a Mamdani fuzzy inference system that uses power error ($\Delta P/\Delta V$) and change in error as inputs to generate optimized duty-cycle corrections according to the rule base. The PSO algorithm depicts the swarm-based MPPT where each particle represents a potential operating point, updated based on global and local bests and the proposed controller integrating hybrid Animated Oat Optimization with an adaptive exploration, exploitation balance and feedback-based reseeding, improving both convergence and tracking accuracy. Each algorithm was interfaced with the wind turbine–PMSG–rectifier–SEPIC subsystem to ensure a fair comparison of MPPT effectiveness.

6.2 Wind speed profile

Figure 9 illustrates the 8-s, wind speed varies between 8 m/s, 9 m/s, 12 m/s, 10 m/s, 9 m/s, 12 m/s, and 10 m/s, simulating dynamic and turbulent wind behavior, input wind velocity profile is deliberately designed to test the performance and adaptability of the MPPT algorithms.

Instead of a smooth or random wind speed, it uses sudden, sharp changes (steps) to see how quickly and accurately each algorithm can find the new maximum power point. Step-change wind profiles were used in this study because they are a widely accepted benchmarking standard for evaluating MPPT controller dynamics in WECS. Such profiles make it possible to clearly observe and compare key transient characteristics such as settling time, overshoot, ripple, and tracking responsiveness which become difficult to isolate when stochastic wind models are used. Prior studies (Borni et al., 2021; Ala et al., 2023; Lopez-Flores et al., 2024) consistently adopt step wind variations for MPPT evaluation, noting that they provide a controlled, repeatable, and fair comparison framework for nonlinear and metaheuristic algorithms. Step inputs also represent worst-case operating transitions, enabling a direct assessment of controller robustness and dynamic stability while simplifying the interpretation of performance metrics. Although stochastic wind models are useful for long-term energy studies, they tend to mask short-term MPPT behavior; therefore, step profiles remain the preferred choice for benchmarking MPPT algorithms and validating controller logic. The simulation starts Time 0–1s: The wind velocity is constant at 8 m/s. This initial period allows the system to stabilize. Time 1s: The wind speed steps up sharply from 8 m/s to 9 m/s. This segment of the study provides a detailed comparison of the behaviors of differing control methods within the simulation environment. The wind profile was manipulated to change a few times to test each controller’s tracking speed. The wind was steady at 9 m/s from 1 s to 2 s. At 2 s, it jumped up to 12 m/s, a large step that really tests the controllers tracking speed. The wind sustained its value from 2 s to 3 s. At 3 s it sharply dropped to 10 m/s and remained steady from 3 s to 5 s, at which point it took another large step back up to 12 m/s. The last piece of the run, from 7 s to 8 s held the wind steady at 11 m/s. In this pattern there are several

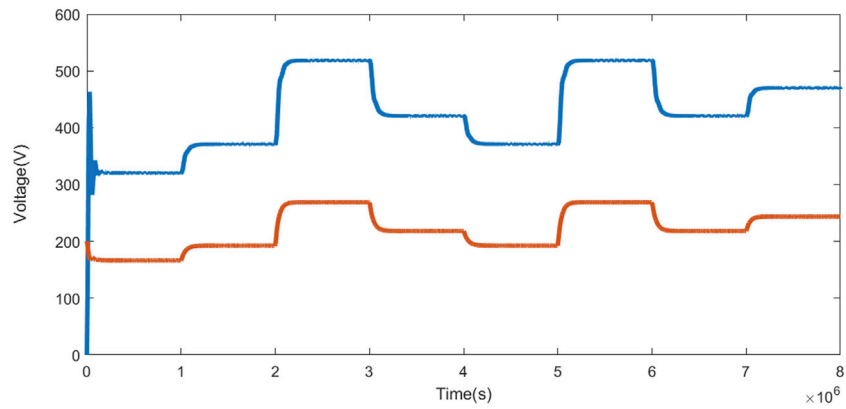


FIGURE 10
Plot of time and voltage.

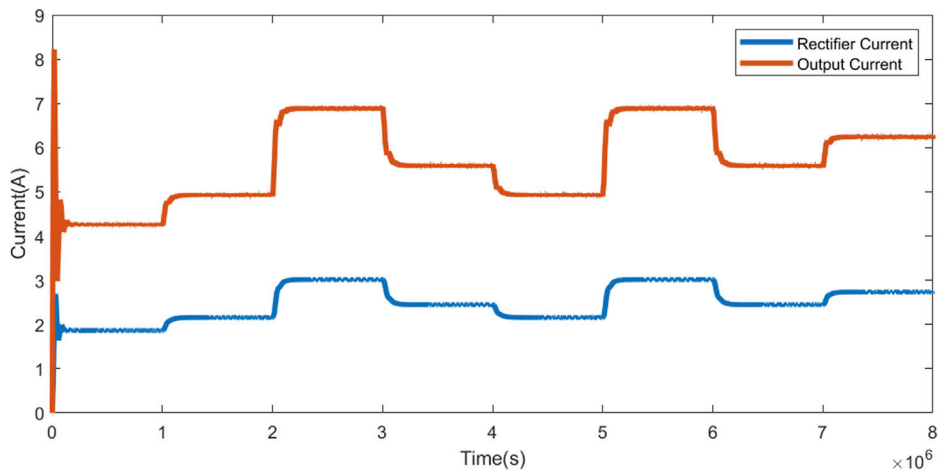


FIGURE 11
Plot of time and current.

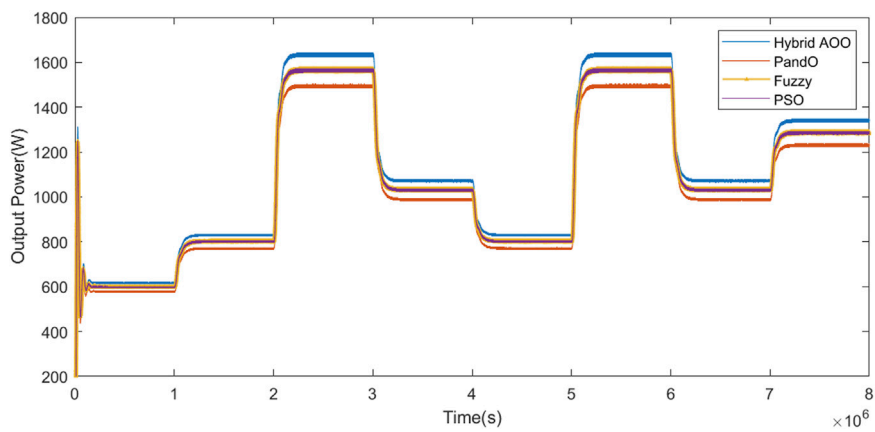


FIGURE 12
Plot of time and output power of AOO, P&O, Fuzzy, and PSO.

TABLE 8 Dynamic and steady-state comparison of P&O and PSO techniques.

Aspect	P&O	PSO
Transient response	Slow, oscillatory	Moderate
Steady-state ripple	High (70 W)	Medium (38 W)
Power stability	Poor	Stable
Adaptability to wind	Weak	Good
Control complexity	Low	High

TABLE 9 Dynamic and steady-state comparison of fuzzy and hybrid AOO techniques.

Aspect	Fuzzy	Hybrid AOO (proposed)
Transient response	Fast	Fastest and smooth
Steady-state ripple	Low (25 W)	Very low (15 W)
Power stability	Stable	Highly stable
Adaptability to wind	Good	Excellent
Control complexity	Medium	Moderate (RT-feasible)

TABLE 10 Key improvements of hybrid AOO over other MPPT controllers.

Metric	vs. P&O	vs. PSO	vs. Fuzzy
Power output gain (%)	+9.30	+4.65	+4.45
Ripple reduction (%)	-78.6	-60.5	-40.0
Settling time reduction (%)	-76.0	-60.0	-52.0
Efficiency gain (%)	+8.27	+4.64	+4.46

up and down transitions allowing the response times of P&O, Fuzzy, PSO, and Hybrid AOO to be seen after every change.

6.3 Voltage characteristics

Figure 10 demonstrates the behaviors of both the converter and load voltages as a result of a changing wind velocity. The rectifier output stays around 250 V, while the load voltage increases with wind speed and reaches roughly 520 V when the wind is 12 m/s.

6.4 Current characteristics

The current behaviour appears in Figure 11. Rectifier current lies between 4 A and 8.5 A, and load current between 2 A and 3 A.

When the wind changes, the Hybrid AOO controller settles the current fastest and shows the smallest overshoot (1.6%) compared with Fuzzy (2.8%), PSO (4.2%), and P&O (8.5%). Its better damping reduces the transient swings, demonstrating that the controller can adapt quickly.

6.5 Output power comparison

At a normal wind speed of 10 m/s, Hybrid AOO produces about 1 642 W, which is higher than Fuzzy (1572 W), PSO (1569 W), and P&O (1502 W). In the second jump in wind speed when it increased to 12 m/s Hybrid AOO reaches the new maximum-power point in only 0.12 s, while P&O is approximately 0.5 s. Figure 12 compares the instantaneous output power of all the algorithms.

Table 6 compares the output power obtained by the four MPPT algorithms P&O, Fuzzy, PSO, and Hybrid AOO at various wind speeds. For every wind speed, power generation increases with wind velocity, but the Hybrid AOO method clearly outperforms the others. At 8 m/s, P&O delivers about 581 W, whereas the AOO reaches 619 W, showing an early advantage of roughly 6%. At the maximum test speed of 12 m/s, AOO achieves 1642 W, compared with 1572 W for Fuzzy, 1569 W for PSO, and 1502 W for P&O. This steady performance gap highlights the faster tracking and stronger adaptability of the Hybrid AOO algorithm under changing wind conditions. This indicates to us that the alternating exploration-and-exploitation logic within the Hybrid AOO helps to identify the correct point faster than the P&O and still maintain the power stable and the bold values in Tables 6, 7 represent the highest output power achieved among the compared MPPT algorithms for each wind speed.

6.6 Quantitative comparison of MPPT algorithms

Theoretical Power is 1692 W using the wind turbine parameters provided in Table 1, Table 7 exhibits the numerical outcomes. Hybrid AOO achieves the greatest average power (1,642 W) and the most effective tracking performance (97.02%). Its steady-state ripple is only 15 W, indicating that the converter remains extremely stable. The settling time is 0.12 s, which is approximately 76% faster than P&O and 60% of PSO. The overshoot is also the lowest at 1.6%, demonstrating a well-damped transient response. In contrast, the P&O algorithm performed the worst due to its continuous perturbation, which causes the system to oscillate around the maximum power point (MPP).

PSO and Fuzzy showed middle-range performances; they were smoother than P&O but slower to react due to a static update of their parameters.

6.7 Dynamic and steady-state comparison

A broader comparison is shown in Table 8 and 9. According to the data, Hybrid AOO provides a fast transient response, low ripple, and adaptive performance under rapid changes in wind speed combined. The PSO and Fuzzy methods remain relatively stable,

but the settling time takes longer due to their iterative model or rule-based approach.

PSO and Fuzzy demonstrated reasonable stability, however, they do take longer to settle due to the limitations of iterative optimisation and rule-based inference. The P&O method was simplistic, however, it could not maintain steady tracking for dynamic conditions, making it inefficient and unstable in operation.

7 Discussion

The comparison of the simulation results indicated that the Hybrid AOO MPPT prevailed over the previous P&O methodology in terms of performance, which was evident simply by examining the plots. As can be seen from the surge in average power to about 9%, the reduction in voltage/current ripple of nearly four-fifths, and settling time also decreased to about one-quarter of the original time. The efficiency of the converter rose slightly over 8%. This increase stemmed largely from two elements within the hybrid AOO: the use of a time-varying optimization factor that speeded the convergence, and the small reseeding step that prevented the search from being stuck in a local point. By combining these two possibilities, the controller was able to navigate to the global maximum quickly, while still remaining stable, real-time operation. Although the wind condition changed abruptly, the system maintained a constant power output, which is impressive and a huge indicator of stability and robustness. Out of every control mechanism studied, the hybrid AOO was the most stable. It had quick response, produced almost no overshoot, and the ripple remained small. The peak power we obtained from the samples taken was about 1642 W, and the efficiency achieved was at a measured 97.02%. These values were the best for any of the tests we conducted.

Returning to Table 10, we see the same results. The average power output increased 9% over the P&O case, which was similar to the 4%–5% increase over the PSO and Fuzzy tests, keeping in mind that we did not attempt a direct comparison between the PSO and Fuzzy tests themselves. The ripple ultimately decreased approximately 80%, indicating that voltage and current maintain a high level of consistency. The time taken to settle was below 50%, which indicates the system was settling faster. The tracking efficiency increased about 4%–8% compared to the previous one, which means that detection of MPP was better, and steady-state errors were smaller. In the end, the hybrid AOO controller was the best performer of any of the tested MPPT techniques, with regards to time to settle, stability, and accuracy.

Overall, all these relative differences proved that hybrid AOO based MPPT had a significantly faster dynamic response (settling time), reduced and oscillation, and higher efficiency of energy capture, when compared to the traditional and intelligent MPPT.

8 Conclusion

This work was undertaken to develop and test an improved control technique for small-scale WECS. This was achieved

considering the detail of the simulation and the hybrid AOO controller showed a great balance of speed and also stability and accuracy. Compared to the P&O, PSO and Fuzzy methods it also led to higher output power, less ripple to maximum-power point and also less time to maximum-power point. The SEPIC converter has enabled us to keep a steady DC-bus voltage and the adaptive AOO logic with respect to wind conditions has demonstrated counter wise behaviour when wind conditions changed rapidly. In future there are a number of potential avenues of extending this work. For example, it should be possible to examine the same control principle in an experimental setup to validate the response with real sensors and actual converter losses. Future iterations may include battery-storage management, operation in grid-connected mode, and hybrid PV-wind systems to understand hybrid AOO operation across multiple energy sources and also we will all stochastic wind behavior. Further developments, potentially through neuro-fuzzy adaptation, reinforcement learning, or multi-objective optimisation will improve convergence speed and long-term stability. After a few more developments, the Hybrid AOO framework, could transform from simulation to a comprehensive, full-scale solution for smart, sustainable energy systems in the field.

Data availability statement

The original contributions presented in the study are included in the article/supplementary material, further inquiries can be directed to the corresponding author.

Author contributions

UK: Conceptualization, Formal Analysis, Investigation, Methodology, Resources, Software, Supervision, Validation, Visualization, Writing – original draft, Writing – review and editing. JH: Conceptualization, Formal Analysis, Methodology, Resources, Supervision, Validation, Visualization, Writing – review and editing.

Funding

The author(s) declared that financial support was received for this work and/or its publication. This research work is supported by the Seed Grant Product Development Scheme (Grant No. SG20210242) of Vellore Institute of Technology, Vellore, India.

Conflict of interest

The author(s) declared that this work was conducted in the absence of any commercial or financial relationships that could be construed as a potential conflict of interest.

Generative AI statement

The author(s) declared that generative AI was not used in the creation of this manuscript.

Any alternative text (alt text) provided alongside figures in this article has been generated by Frontiers with the support of artificial intelligence and reasonable efforts have been made to ensure accuracy, including review by the authors wherever possible. If you identify any issues, please contact us.

References

- Aboras, K. M., EL-Banna, M. H., Megahed, A. I., and Hammad, M. R. (2025). Optimal maximum power point tracking strategy based on greater cane rat algorithm for wind energy conversion system. *Sci. Rep.* 15, 1–21. doi:10.1038/s41598-025-18710-7
- Ala, A., Mahmoudi, A., Mirjalili, S., Simic, V., and Pamucar, D. (2023). Evaluating the performance of various algorithms for wind energy optimization: a hybrid decision-making model. *Expert Syst. Appl.* 221, 119731. doi:10.1016/j.eswa.2023.119731
- Ali, M. O., and Ahmad, A. H. (2020). Design, modelling and simulation of controlled sepic dc-dc converter-based genetic algorithm. *Int. J. Power Electron. Drive Syst.* 11, 2116–2125. doi:10.11591/ijpeds.v11.i4.pp2116-2125
- Alsumiri, M., and Althomali, R. (2017). Implementation of sepic in small scale wind power generation system. *Eng. Energy Technol.* 3, 153–162. doi:10.20319/mijst.2017.32.153162
- Arabi, M., Zennir, Y., and Bounezour, H. (2024). “Enhancing mppt control of variable wind turbines: a comparative study of optimal pi controllers with the novel gjo algorithm and the pso and hho algorithms,” in *Proceedings of the 2024 international conference on advanced electrical communication technologies (ICAECOT)*, 1–6. doi:10.1109/ICAECOT62402.2024.10994847
- Borni, A., Bechouat, M., Bessous, N., Bouchakour, A., Zaarour, L., and Zaghba, L. (2021). Comparative study of p&o and fuzzy mppt controllers and their optimization using pso and ga to improve wind energy system. *Int. J. Eng. Model.* 34, 55–76. doi:10.31534/engmod.2021.2.ri.05d
- Eldodor, M. M., Mousa, M. A., Farrag, A. A., and El-Deib, A. (2020). “Small wind turbine design and implementation using mppt current control,” in *Proceedings of the 6th IEEE international energy conference (ENERGYCon)*, 556–561. doi:10.1109/ENERGYCon48941.2020.9236586
- Emar, W., Attar, H., Saraereh, O. A., Qabaja, M., and Fares, O. (2024). An oppt for a pmsg with a new sepic-buck converter for a wind-driven pmsg system used in rural areas. *Int. J. Appl. Sci. Eng.* 21. doi:10.6703/IJASE.202406_21(2).003
- Eswaraiah, B., and Balakrishna, K. (2024). Design and development of different adaptive mppt controllers for renewable energy systems: a comprehensive analysis. *Sci. Rep.* 14, 21627. doi:10.1038/s41598-024-72861-7
- Hannan, M. A., Al-Shetwi, A. Q., Mollik, M. S., Ker, P. J., Mannan, M., Mansor, M., et al. (2023). Wind energy conversions, controls, and applications: a review for sustainable technologies and directions. *Sustainability* 15, 3986. doi:10.3390/su15053986
- Hussain, J., and Mishra, M. K. (2014). “Adaptive mppt control algorithm for small-scale wind energy conversion systems,” in *2014 IEEE international conference on power electronics, drives and energy systems (PEDES)*, 1–5. doi:10.1109/PEDES.2014.7042085
- Jyothi, B., Bhavana, P., Rao, B. T., Pushkarna, M., and Djidimbele, R. (2023). Implementation of modified sepic converter for renewable energy built dc microgrids. *Int. J. Photoenergy* 2023, 1–13. doi:10.1155/2023/2620367
- Karthikeyan, U., and Hussain, J. (2025). Enhancing the efficiency of wind energy conversion systems using novel airfoil based small scale wind turbine. *Rev. Matéria* 30, e20240827. doi:10.1590/1517-7076-RMAT-2024-0827
- Kennedy, R., and Eberhart, J. (2021). Particle swarm optimisation. *Stud. Comput. Intell.* 927, 5–13. doi:10.1007/978-3-030-61111-8_2
- Kumari, R., Dahal, R., Pandit, M., and Sherpa, K. S. (2024). A single-switch high-gain cascaded boost–sepic converter using small wind turbine for renewable energy applications. *J. Institution Eng. (India) Ser. B* 105, 1527–1535. doi:10.1007/s40031-024-01061-8
- López Seguel, J., Seleme, I. S. J., and Morais, L. M. F. (2022). Comparative study of buck-boost, sepic, cuk and zeta dc-dc converters using different mppt methods for photovoltaic applications. *Energies* 15, 7936. doi:10.3390/en15217936
- Lopez-Flores, D. R., Acosta-Cano-De-Los-Rios, P. R., Marquez-Gutierrez, P. R., Acosta-Cano-De-Los-Rios, J. E., Baray-Arana, R. E., and Ramirez-Alonso, G. (2024). Efficient and fast wind turbine mppt algorithm using ts fuzzy logic and optimal relation methods. *IEEE Lat. Am. Trans.* 22, 612–619. doi:10.1109/TLA.2024.10562259
- Mejbel, I. A., and Hassan, T. K. (2023). Design and simulation of high gain sepic Dc–Dc converter. *J. Eng. Sustain. Dev.* 27, 138–148. doi:10.31272/jeasd.27.1.12
- Pande, J., Nasikkar, P., Kotecha, K., and Varadarajan, V. (2021). A review of maximum power point tracking algorithms for wind energy conversion systems. *J. Mar. Sci. Eng.* 9, 1–30. doi:10.3390/jmse9111187
- Pande, J. A., Nasikkar, P., Kotecha, K., and Abraham, A. (2024). An ingenious technique to track the maximum power point for a wind energy system. *IEEE Access* 12, 10160–10171. doi:10.1109/ACCESS.2024.3354708
- Rashmi, G., and Linda, M. M. (2023). A novel mppt design for a wind energy conversion system using grey wolf optimization. *Automatika* 64, 798–806. doi:10.1080/00051144.2023.2218168
- Ravi, S., Premkumar, M., and Abualigah, L. (2023). Comparative analysis of recent metaheuristic algorithms for maximum power point tracking of solar photovoltaic systems under partial shading conditions. *Int. J. Appl. Power Eng.* 12, 196–217. doi:10.11591/ijape.v12.i2.pp196-217
- Sarathi, J., and Rama Prabha, D. (2025). An effective anfis approach for interconnected dfng-based wind energy system with model-in-loop validation. *IEEE Access* 13, 77147–77164. doi:10.1109/ACCESS.2025.3565073
- Stadtherr, A. (2019). Cornerstone: a collection of scholarly and creative works – reading comprehension in the secondary classroom
- Sutikno, T., and Aprilianto, R. A. (2023). Application of sepic dc-dc converter for low-voltage energy harvesting systems. *Energy Harvest. Syst.* 1, 1–7. doi:10.11591/ehs.v1i1.pp1-7
- Tan, K., and Islam, S. (2004). Optimum control strategies in energy conversion of pmsg wind turbine system without mechanical sensors. *IEEE Trans. Energy Convers.* 19, 392–399. doi:10.1109/TEC.2004.827038
- Teklehaimanot, Y. K., Akingbade, F. K., Ubochi, B. C., and Ale, T. O. (2024). A review and comparative analysis of maximum power point tracking control algorithms for wind energy conversion systems. *Int. J. Dyn. Control* 12, 3494–3516. doi:10.1007/s40435-024-01434-3
- Vendoti, S., Sekhar, A. H., Bharadwaja, A. V., Kommula, B. N., Sateesh, R., Prabhakar, S., et al. (2025). Grid connected improved sepic converter with intelligent mppt strategy for energy storage system in railway applications. *Sci. Rep.* 15, 1–27. doi:10.1038/s41598-025-96704-1
- Vu, N. T. T., Nguyen, H. D., and Nguyen, A. T. (2022). Reinforcement learning-based adaptive optimal fuzzy mppt control for variable speed wind turbine. *IEEE Access* 10, 95771–95780. doi:10.1109/ACCESS.2022.3205124
- Wang, R. B., Hu, R. B., Geng, F. D., Xu, L., Chu, S. C., Pan, J. S., et al. (2025). The animated oat optimization algorithm: a nature-inspired metaheuristic for engineering optimization and a case study on wireless sensor networks. *Knowledge-Based Syst.* 318, 113589. doi:10.1016/j.knsys.2025.113589

Publisher's note

All claims expressed in this article are solely those of the authors and do not necessarily represent those of their affiliated organizations, or those of the publisher, the editors and the reviewers. Any product that may be evaluated in this article, or claim that may be made by its manufacturer, is not guaranteed or endorsed by the publisher.